Overexpression of sterol carrier protein-2 differentially alters hepatic cholesterol accumulation in cholesterol-fed mice

Barbara P. Atshaves,* Avery L. McIntosh,* Gregory G. Martin,* Danilo Landrock,† H. Ross Payne,† Shivaprasad Bhuvanendran,* Kerstin K. Landrock,* Olga I. Lyuksyutova,* Jeffery D. Johnson,§ Ronald D. Macfarlane,§ Ann B. Kier,† and Friedhelm Schroeder[1,*]

Departments of Physiology and Pharmacology,* Pathobiology,† and Chemistry,§ Texas A&M University, Texas Veterinary Medical Center, College Station, TX 77843-4466

Abstract **Although in vitro studies suggest a role for sterol carrier protein-2 (SCP-2) in cholesterol trafficking and metabolism, the physiological significance of these observations remains unclear. This issue was addressed by examining the response of mice overexpressing physiologically relevant levels of SCP-2 to a cholesterol-rich diet. While neither SCP-2 overexpression nor cholesterol-rich diet altered food consumption, increased weight gain, hepatic lipid, and bile acid accumulation were observed in wild-type mice fed the cholesterol-rich diet. SCP-2 overexpression further exacerbated hepatic lipid accumulation in cholesterol-fed females (cholesterol/cholesteryl esters) and males (cholesterol/cholesteryl esters and triacyglycerol). Primarily in female mice, hepatic cholesterol accumulation induced by SCP-2 overexpression was associated with increased levels of LDL-receptor, HDL-receptor scavenger receptor-B1 (SR-B1) (as well as PDZK1 and/or membrane-associated protein 17 kDa), SCP-2, liver fatty acid binding protein (L-FABP), and 3α-hydroxysteroid dehydrogenase, without alteration of other proteins involved in cholesterol uptake (caveolin), esterification (ACAT2), efflux (ATP binding cassette A-1 receptor, ABCG5/8, and apolipoprotein A1), or oxidation/transport of bile salts (cholesterol 7α-hydroxylase, sterol 27α-hydroxylase, Na^+/taurocholate cotransporter, Oatp1a1, and Oatp1a4). The effects of SCP-2 overexpression and cholesterol-rich diet was downregulation of proteins involved in cholesterol transport (L-FABP and SR-B1), cholesterol synthesis (related to sterol regulatory element binding protein 2 and HMG-CoA reductase), and bile acid oxidation/transport (via Oapt1a1, Oatp1a4, and SCP-x). Levels of serum and hepatic bile acids were decreased in cholesterol-fed SCP-2 overexpression mice, especially in females, while the total bile acid pool was minimally affected.** **Taken together, these findings support an important role for SCP-2 in hepatic cholesterol homeostasis.**—Atshaves, B. P., A. L. McIntosh, G. G. Martin, D. Landrock, H. R. Payne, S. Bhuvanendran, K. K. Landrock, O. I. Lyuksyutova, J. D. Johnson, R. D. Macfarlane, A. B. Kier, and F. Schroeder. **Overexpression of sterol carrier protein-2 differentially alters hepatic cholesterol accumulation in cholesterol-fed mice.** ***J. Lipid Res.*** **2009.** 50: **1429–1447.**

Supplementary key words liver fatty acid binding protein • transgenic mice • cholesterol

Due to the deleterious effects associated with cholesterol accumulation leading to atherosclerosis, levels of cholesterol in cells and tissues are carefully regulated (1, 2). Cholesterol is derived from both diet and endogenous synthesis, and in order to maintain cholesterol homeostasis, human liver excretes nearly 2 g of cholesterol per day into bile (3). Decreased cholesterol disposal results in hepatic cholesterol accumulation and elevated blood cholesterol, while excessive cholesterol secretion or disproportionate biliary constituents may lead to cholelithiasis and inflammatory gallbladder disease (3, 4). Cholesterol is removed from peripheral tissues to the liver for elimination by oxidation and/or biliary excretion via a process termed reverse cholesterol transport (RCT). Recent novel experiments have elucidated many molecular details of the RCT pathway, including those involving scavenger receptor-B1 (SR-B1)-mediated uptake of HDL-cholesteryl esters and ABC transporter-

This work was supported in part by the U.S. Public Health Service, National Institutes of Health Grants GM31651 (F.S. and A.B.K.), DK41402 (F.S. and A.B.K.), and DK70965 (B.P.A.). The helpful technical assistance of Ms. Meredith Dixon was much appreciated.

Manuscript received 21 January 2009 and in revised form 12 March 2009.

Published, JLR Papers in Press, March 16, 2009.
DOI 10.1194/jlr.M900020-JLR200

Abbreviations: 3α-HSD, 3α-hydroxysteroid dehydrogenase; ABCA-1, ATP binding cassette A-1 receptor; apoA1, apolipoprotein A1; CYP27A1, sterol 27α-hydroxylase; CYP7A1, cholesterol 7α-hydroxylase; L-FABP, liver fatty acid binding protein; LXR-α, liver X receptor-α; MAP-17, membrane-associated protein 17 kDa; Ntcp, Na^+/taurocholate cotransporter; Oatp, organic anion transporting polypeptide 1; PDZK1, postsynaptic density protein/*Drosophila* disc large tumor suppressor (dlg)/tight junction protein (ZO1); RCT, reverse cholesterol transport; SCP, sterol carrier protein; SHP, short heterodimer partner; SR-B1, scavenger receptor-B1; SREBP-2, sterol regulatory element binding protein 2; WT, wild type.

[1] To whom correspondence should be addressed.
e-mail: fschroeder@cvm.tamu.edu

mediated cholesterol efflux via ATP binding cassette A-1 receptor (ABCA-1), ABCG1, and ABCG5/8 (reviewed in Refs. 3–8). In contrast, much less is known regarding the mechanism(s) whereby unesterified cholesterol leaves the plasma membrane for transfer through the cytoplasm to the bile canaliculus for efflux. While the ability of cytoplasmic cholesterol binding protein(s), such as sterol carrier protein-2 (SCP-2), to facilitate cholesterol uptake and transhepatocyte transfer has been shown, this work was undertaken to study the process of cholesterol homeostasis in transgenic mice stably overexpressing physiologically relevant levels of SCP-2 in response to a cholesterol-rich diet. The working hypothesis is that SCP-2, as a cholesterol transport protein, plays an important role in cholesterol homeostasis by affecting hepatic lipid and protein expression through its association with other proteins involved in cholesterol metabolism. Key physiological questions to be answered by this study include how SCP-2 upregulation or overexpression affects the hepatic and serum cholesterol phenotype, especially in the presence of a cholesterol-rich diet. The rationale for studying cholesterol homeostasis in a SCP-2 overexpression mouse model is clear from the extensive literature establishing SCP-2 as a major player in cholesterol homeostasis through uptake and transhepatocyte transfer (9–13).

Both in vitro and imaging studies have detected SCP-2 in plasma membrane cholesterol-rich microdomains in both caveolin-1-expressing (L-cell fibroblasts) and caveolin-1-deficient (hepatocytes) cells (14, 15). In addition, SCP-2 directly interacts with plasma membrane cholesterol-rich microdomain proteins (e.g., caveolin-1) involved in cholesterol uptake/trafficking (16, 17). Based on SCP-2's localization in and interactions with proteins in cholesterol-rich microdomains, as well as its high affinity for cholesterol (K_d up to 4 nM), SCP-2 is hypothesized to facilitate cholesterol desorption from the plasma membrane and/or endocytic vesicles into the cytoplasm to facilitate uptake (reviewed in Refs. 8 and 18). Consistent with this hypothesis, SCP-2 enhanced intermembrane sterol transfer—preferentially from cholesterol-rich but not cholesterol-poor microdomains (reviewed in Refs. 8, 19, and 20). In vitro studies showed that SCP-2 stimulated cholesterol metabolism to cholesteryl esters, steroid hormones, and 7a-hydroxycholesterol (necessary for bile acid synthesis) (reviewed in Ref. 18). In cultured fibroblasts, SCP-2 overexpression enhanced cholesterol uptake, stimulated cholesterol intracellular retention by increasing esterification and decreasing efflux, facilitated intracellular cholesterol cycling, and altered the properties of plasma membrane lipid cholesterol-rich microdomains wherein the SR-B1 and several ABC transporters are localized (reviewed in Refs. 8, 15, and 18).

While these and other studies (9–13) suggest a role for SCP-2 in hepatic cholesterol homeostasis, the full physiological significance remains unclear. The key physiological questions to be answered by this work include how sex, diet, and SCP-2 overexpression affect lipid levels and proteins involved in cholesterol homeostasis. To begin to resolve this issue, a stable SCP-2 overexpression mouse model (20+ generations) was produced by pronuclear injection. The effects of a cholesterol-rich diet on male and female mice were examined to show that, depending on sex and diet, SCP-2 overexpression significantly *i*) potentiated the effect of cholesterol on increased body weight gain, especially in female mice; *ii*) increased hepatic mass and lipid (cholesterol and cholesteryl esters) accumulation, more so in females; and *iii*) increased hepatic expression of proteins involved in cholesterol uptake and intracellular trafficking, especially those proteins involved in the RCT pathway. Taken together, these results indicate a significant role for SCP-2 in hepatic cholesterol metabolism.

MATERIALS AND METHODS

Materials

Silica Gel G TLC plates were from Analtech (Newark, DE). Lipid standards were purchased from Nu-Chek Prep (Elysian, MN). Rabbit polyclonal antibodies directed against mouse SCP-2 (recognizing 58 kDa SCP-x, 15 kDa pro-SCP-2, and 13.2 kDa SCP-2) and rat liver fatty acid binding protein (L-FABP) were prepared as described earlier (21, 22). Rabbit polyclonal antibodies were purchased from the following sources: anticaveolin-1 from BD Transduction Laboratories (Lexington, KY); anti-3α-hydroxysteroid dehydrogenase from USBiological (Swampscott, MA); anti-ABCA-1 and anti-SR-B1 from Novus Biologicals (Littleton, CO); anti-sterol regulatory element binding protein 1 (SREBP-1), anti-membrane-associated protein 17 kDa (MAP-17), and postsynaptic density protein/*Drosophila* disc large tumor suppressor (dlg)/tight junction protein (ZO1) (PDZK1) from Santa Cruz Biotechnology (Santa Cruz, CA); anti-HMG-CoA reductase from Upstate Cell Signaling Solutions (Lake Placid, NY); and anti-ACAT2 from Cayman Chemical (Ann Arbor, MI). Goat polyclonal antibodies were purchased from the following sources: anti- LDL-receptor, anti-cholesterol 7α-hydroxylase (CYP7A1), anti-sterol 27-hydroxylase (CYP27A1), anti-liver X receptor-α (LXR-α), and anti-short heterodimer partner protein (SHP) were purchased from Santa Cruz Biotechnology. Monoclonal anti-GAPDH was from Millipore (Billerica, MA). All reagents and solvents used were of the highest grade available and were cell culture tested as necessary.

Animal care

Adult male and female (2 months of age, 20–30 g) inbred FVB/Ncrl (Friend Virus B/NIH Charles River 1) mice were obtained from the National Cancer Institute (Frederick Cancer Research and Developmental Center, Maryland). Except when on the cholesterol diet, all mice were maintained on a standard rodent chow mix (5% calories from fat). Mice were kept under a 12 h light/dark cycle in a temperature-controlled (25°C) facility with access to food and water ad libitum. Mice in the facility were monitored quarterly for infectious diseases and were specific pathogen free. Animal protocols were approved by the Animal Care and Use Committee of Texas A&M University.

Creation of SCP-2 transgenic mice

Transgenic mice stably overexpressing SCP-2 (20+ generations) were produced by pronuclear microinjection on a FVB/Ncrl background strain according to standard protocols (23). The SCP-2 expression construct was prepared as follows: mouse SCP-2 cDNA was generated using the 1st-strand™ cDNA Synthesis Kit from Clontech (Palo Alto, CA) with total RNA prepared as described in (24). The 1st-strand SCP-2 cDNA was amplified using the *Pfu* DNA polymerase from Stratagene (La Jolla, CA) under conditions optimized for high-fidelity DNA synthesis. Primers were designed with the following restriction enzyme sites: *Kpn*I (start) and *Xho*I

(halt) for easy ligation into the mammalian expression plasmid pKJ1DF (PGK), a generous gift from Dr. M. McBurney, Texas A&M University. The PGK vector, under the control of the *Pgk* promoter with 5′ and 3′ untranslated regions included, was used in the development of the pronuclear expression construct for SCP-2 overexpression since control regions upstream and downstream of the constitutively expressed mouse *Pgk*-1 gene (encoding for phosphoglycerate kinase) were shown to promote expression of the coding regions in various mammalian cells (25, 26). DNA sequencing was performed to verify identity and fidelity. The *Eco*RI-*Bgl*II DNA fragment from the expression construct was injected into the pronucleus of mouse embryos and transferred into pseudopregnant recipient mice to generate transgenic mice overexpressing SCP-2. The presence of the transgene was verified by Southern blot analysis and PCR screening. Protein levels of SCP-2 were determined by Western blot analysis and shown to be stable to date (20+ generations). To ensure that any observed phenotypic changes were not the result of random SCP-2 cDNA insertion, three SCP-2 overexpression mouse lines were screened and assayed for SCP-2 levels. Since all three strains exhibited similar trends in protein expression and lipid content with no observed morphologic phenotypic differences, only one strain was expanded for subsequent analysis. One copy of the transgene was integrated into the genome as determined by the Genetic Testing Services at Charles River Laboratories (Troy, NY) using real-time PCR on tail genomic DNA from heterozygous transgenic mice (n = 6). While multiple copy numbers were not observed, the literature contains many examples of single-copy transgenes with variable levels of protein expression, and often, multiple copy integration patterns are associated with low protein expression due to gene silencing at the transcriptional level (27, 28).

Dietary (cholesterol) studies

Mice were maintained as a FVB/Ncrl inbred strain with wild-type (WT) breeders directly obtained from the original stock at the National Cancer Institute from the Frederick Cancer Research and Developmental Center. Since WT littermates of SCP-2 overexpression mice on the FVB/Ncrl background did not significantly differ in terms of lipid or protein analysis from inbred FVB/Ncrl mice of matching age/sex obtained from the same National Cancer Institute stock used in developing the overexpressing strain, both WT littermates and FVB/Ncrl mice of matching sex/age were used as control animals in the feeding studies. One week before beginning the dietary studies, male and female mice (2 month of age, 20–30 g) were transferred to a modified AIN-76A phytoestrogen-free control diet (5% calories from fat; D11243, Research Diets, New Brunswick, NJ). This diet was free from any significant amounts of cholesterol and/or phytoestrogens (29) that could complicate any cholesterol-effect and sex-based comparisons (30). Each mouse was housed individually in Techniplast Sealsafe™ IVC cages with external water bottles and wire bar lid holders containing food pellets. After 1 week, half of the mice remained on the control diet, while the rest were transferred to a modified AIN-76A rodent diet supplemented with 1.25% cholesterol (5% calories from fat; Diet D01091702, isocaloric to control diet, Research Diets). Mouse body weights and food intake were monitored every other day as follows: at similar times of the day (midmorning), each mouse was removed from the cage, placed in a beaker, and weighed. To measure food intake, remaining pellets from the food holder and bedding (strained to gather smaller pellets that had fallen through the lid mesh) were weighed. Since the food was color-coded (yellow for control food and blue for 1.25% cholesterol), pellets were clearly visible and not easily missed. At the end of the study (day 28), animals were fasted overnight (to assure liver lipids were not influenced by recent digestion, resulting in better uniformity in lipid analysis), anesthetized (ketamine 100 mg/kg; zylaxine 10 mg/kg), and blood collected by cardiac puncture. The anesthetized mice were then euthanized by cervical dislocation, and livers were harvested and weighed. Liver slices were excised for morphological examination of lipid droplets with remaining portions snap-frozen on dry ice and stored at −80°C for lipid and Western analyses as described in (22).

Morphometric measurements of hepatic lipid droplets

Liver samples (25 to 75 mm^3 segments) were fixed by immersion in 4% formaldehyde at room temperature. Lipid droplets in the liver samples were stained by a histological procedure described earlier (31), with slight modifications. Briefly, liver tissue was incubated for 9 h in 1% osmium tetroxide and 2.5% potassium dichromate, dehydrated in a graded ethanol series, and embedded in Spurr's epoxy resin. Semithin sections, 0.75 μm thick, were mounted on glass slides, coverslipped and examined without counterstaining. These liver sections with darkly stained lipid droplets were imaged with a 20× light microscope objective and recorded with a CCD camera. Representative images were randomly selected from each liver for a total image area of 2.5 to 6.2 mm^2 per treatment group. The percentage area of lipid droplets in the image field was analyzed with the program ImageJ (developed at the U.S. National Institutes of Health and available at http://rsb.info.nih.gov/ij/).

Lipid mass

Hepatic lipids from male and female WT and SCP-2 overexpression mice on control and cholesterol (1.25%) diets were extracted with *n*-hexane-2-propanol 3:2 (v/v) (32) and immediately stored under an atmosphere of N_2 to limit oxidation. Protein content was determined by the method of Bradford (33) from the dried protein residue digested overnight in 0.2 M KOH. Lipid classes (cholesterol, free fatty acid, triacylglycerol, cholesterol ester, and phospholipid) were resolved using silica gel G TLC plates developed in a solvent system of petroleum ether/diethyl ether/methanol/acetic acid (90:7:2:0.5) (34). Lipids were identified by comparison to known standards. TLC spots were visualized by iodine, scraped, and quantitated by the method of Marzo et al. (35). All glassware was prewashed with sulfuric acid-chromate.

Lipid and bile acid content in liver, serum, and gall bladder

Total bile acid content from the mouse liver homogenate, serum, and gall bladder was determined using the commercially available Bile Acids-L3K assay kit (Diagnostic Chemicals, Oxford, CT) according to the manufacturer's directions as described earlier (36, 37). Biliary cholesterol was determined with kit no. 274-47109 (Wako Diagnostics, Richmond, VA) using cholesterol as a standard. Since phosphatidylcholine is the major biliary phospholipid and 2-linoleoyl-1-palmitoyl-*sn*-glycero-3-phosphocholine is the major phosphatidylcholine species, biliary phospholipids were quantified with kit no. 990-54009 (Wako Diagnostics) using 2-linoleoyl-1-palmitoyl-*sn*-glycero-3-phosphocholine (Sigma-Aldrich) as a standard. Biliary bile acid, cholesterol, and phospholipid content were expressed as mmol/L. Serum total cholesterol (Wako 276-64909), phospholipid (Wako 990-54009), and bile acids (Wako Bile Acids-L3K Assay) were determined with the above Wako kits (Diagnostic Chemicals). Phospholipids were quantified using 2-linoleoyl-1-palmitoyl-*sn*-glycero-3-phosphocholine (Sigma-Aldrich) as standard since this phosphatidylcholine is the most common murine bile phospholipid.

Lipoprotein analysis

In order to determine the effect of SCP-2 expression and cholesterol-rich diet on the serum lipoprotein profile, a Cs_2CdEDTA

density gradient ultracentrifugation method was used to separate serum into VLDL, LDL, and HDL fractions as described in (38). In brief, NBD (C6-ceramide) was added to serum samples to label the lipoproteins, and the solution was applied to a 0.300 M Cs_2CdEDTA density buffer. These samples were spun for 6 h at 120,000 rpm and 5°C in a Beckman OptimaTM TLX-120 Ultracentrifuge equipped with a 30° fixed angle TLA 120.2 rotor. A custom-built fluorescence imaging system was used to measure the distribution of the lipoprotein particles in the ultracentrifuge tubes after the spin as described in (38). The tubes were then frozen on liquid nitrogen and cut in sections based on density measurements to isolate VLDL, LDL, and HDL fractions. Total cholesterol was measured in each fraction using the Wako serum total cholesterol kit (276-64909; Diagnostic Chemicals).

Western blotting

Levels of SCP-2 in the liver, kidney, heart, brain, and intestine from control-fed male and female WT and SCP-2 overexpression mice were determined by Western blotting as described in (22). In order to determine whether SCP-2 overexpression and/or a cholesterol-rich diet altered levels of key proteins involved in lipid metabolism, protein levels in male and female WT and SCP-2 overexpression mice on control and cholesterol (1.25%) diets were measured by Western blotting as described in (22) in the following groups: *i*) proteins that bind/transport cholesterol and bile acids, including SCP-2, L-FABP, caveolin-1, and 3α-hydroxysteroid dehydrogenase (3α-HSD); *ii*) proteins involved in cholesterol uptake, efflux, and storage, such as LDL-receptor, SR-B1, PDZK1, MAP-17, ABCA-1, apolipoprotein A1 (apoA1), and ACAT2; and *iii*) enzymes and nuclear receptors involved in cholesterol and bile acid synthesis, including HMG-CoA reductase, CYP7A1, CYP27A1, SCP-x, LXR-α, and SHP. To ensure equal loading, expression of each protein was normalized to the mean expression of GAPDH. Briefly, since each protein of interest and the housekeeping gene GAPDH was easily resolved by size on the tricine gels, the membranes were cut into two so that each Western blot was probed with antisera against the protein of choice and GAPDH. Proteins were quantified by densitometric analysis after image acquisition using a single-chip CCD video camera and a computer workstation (IS-500 system from Alpha Innotech, San Leandro, CA) (22). Image files were analyzed (mean 8-bit gray-scale density) using ImageJ. For quantitative analysis, linear standard curves were generated from Western blots where pure protein was available (SCP-2, SCP-x, and L-FABP). Band intensities on the Western blots were analyzed as described above and then plotted against protein amount to generate a standard curve within the linear range of each protein. Changes in protein expression were quantitated by comparing the sample to the standard curve on each blot. Proteins with no source of pure protein available were expressed as fold differences between samples.

Real-time PCR

Real-time PCR was performed on total RNA from liver, kidney, heart, brain, and intestine isolated and purified using the RNeasy mini kit (Qiagen,Valencia, CA) in accordance with the manufacturer's protocol. RNA concentrations were determined spectrophotometrically, and integrity was verified by agarose electrophoresis and ethidium bromide staining. For quantitative real-time PCR, expression patterns were analyzed with an ABI PRISM 7000 sequence detection system (Applied Biosystems, Foster City, CA) using TaqMan® One-Step PCR Master Mix Reagent kit, gene-specific TaqMan® PCR probes and primers, and the following thermal cycler protocol: 48°C for 30 min, 95°C for 10 min before the first cycle, 95°C for 15 s, and 60°C for 1 min, repeated 40 times. Using the TaqMan® One-Step chemistry, total RNA was reverse-transcribed in the first step of the thermal cycler protocol (48°C for 30 min) prior to amplification. For specific probes and primers, Assay-on-Demand® products for mouse SCP-2 (Mm001257981_m1), ABCG5 (Mm01226965_m1), ABCG8 (Mm00445977_m1), Cyp7A1 (Mm00484152_m1), HMG-CoA reductase (Mm01282492_m1), Na^+/taurocholate cotransporter (Ntcp; Mm01302718_m1), SREBP-2 (CpT1, Mm01306289_m1), organic anion transporting polypeptide 1 (Oatp1a1; Mm01267414_m1), and Oatp1a4 (Mm00460672_m1) were obtained from Applied Biosystems. Experiments were performed in triplicate and analyzed with ABI Prism 7000 SDS software (Applied Biosystems) to determine the threshold cycle (C_T) from each well. Primer concentrations and cycle number were optimized to ensure that reactions were analyzed in the linear phase of amplification. To analyze the real-time PCR data, mRNA expression of SCP-2, ABCG5, ABCG8, CYP7A1, HMG-CoA reductase, Ntcp, SREBP-2, Oatp1a1, and Oatp1a4 in the different mice groups, including female WT mice on control diet, male/female SCP-2 overexpressing mice on the control diet, male/female WT mice on the cholesterol-rich diet, and male/female SCP-2-overexpressing mice on the cholesterol-rich diet, were normalized to a housekeeping gene (18S RNA) and were made relative to the control mouse group (male WT mice on control diet). Relative expression were calculated using the comparative $2^{-\Delta\Delta CT}$ method (39), where $\Delta\Delta C_T = [C_T \text{ of target gene} - C_T \text{ of 18s}]_{\text{different mice groups}} - [C_T \text{ of target gene} - C_T \text{ of 18s}]_{\text{control mouse group}}$ as described in User Bulletin 2, ABI Prism 7000 Sequence Detection System (Applied Biosystems).

Statistics

Each feeding group consisted of six male and six female animals. All values were expressed as the mean ± SEM. Statistical analysis was performed using ANOVA combined with the Newman-Keuls multiple comparisons test (GraphPad Prism, San Diego, CA). Values with $P < 0.05$ were considered statistically significant.

RESULTS

Generation of SCP-2 overexpression transgenic mice

To ensure that any observed phenotypic changes were not the result of random SCP-2 cDNA insertion, three SCP-2 overexpression strains were generated and initially screened. All three strains exhibited similar trends in protein expression and lipid content with no observed morphologic phenotypic differences. Therefore, only one strain was expanded for subsequent dietary feeding studies. The presence of the transgene (*Eco*RI-*Bgl*II DNA fragment shown in **Fig. 1A**) was confirmed by PCR (Fig. 1B) and Southern blot analysis (Fig. 1C) using primers and probes unique to the transgene. Since the PGK promoter used in the transgene construct was ubiquitous, levels of SCP-2 in various tissues, including liver, kidney, heart, brain, and intestine, were determined by quantitative analysis of multiple Western blots (**Fig. 2A–E**) and RT-PCR analysis (Fig. 2F–J). Protein and mRNA expression levels of SCP-2 in liver (Fig. 2A, F) and kidney (Fig. 2B, G) in the SCP-2-overexpressing male and female mice showed similar fold (1.9- to 2.3-fold, $P \leq 0.05$) increases compared with the WT counterparts. In contrast, no significant increase in protein or mRNA levels of SCP-2 in heart (Fig. 2C, H), brain (Fig. 2D, I), or intestine (Fig. 2E, J) were observed.

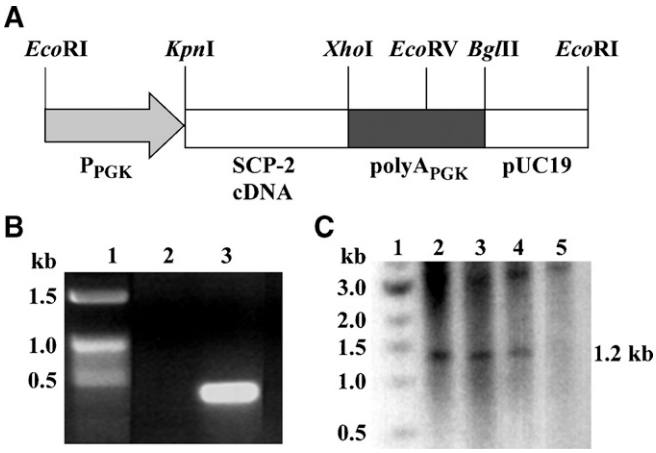

Fig. 1. Generation of the SCP-2 transgenic mouse. The SCP-2 expression construct (A) included the entire coding region of mouse 15 kDa pro-SCP-2 subcloned into plasmid pKJ1DF from which the *Eco*RI/*Bgl*II fragment was microinjected into mouse embryo pronuclei to establish SCP-2-overexpressing mice. A PCR screen (B) was designed to detect the presence of the transgene in tail DNA from WT (lane 2) and SCP-2- overexpressing (lane 3) mice. Southern blot analysis (C) of *Eco*RV/*Eco*RI-digested DNA was performed to show the 1.2 kb transgene in three different lines of SCP-2 transgenic (lanes 2–4) but not WT (lane 5) mice.

Effect of SCP-2 overexpression and cholesterol-rich diet on hepatic SCP-2 and SCP-x expression

Since SCP-2 is most highly expressed in liver, Western blot analysis was performed for multiple transgenic and WT littermate controls from the livers of control and cholesterol-fed male and female mice to evaluate transgene expression (**Fig. 3**). Consistent with complete posttranslational cleavage of 15 kDa pro-SCP-2, Western blotting detected only the mature 13.2 kDa SCP-2 protein in liver homogenates (Fig. 3C, D). Quantitative analysis of multiple Western blots (normalized to the housekeeping gene GAPDH) revealed hepatic levels of SCP-2 in control-fed male and female SCP-2 overexpression mice increased 1.9- and 2.3-fold, respectively (Fig. 3A, $P \leq 0.02$) as compared with WT counterparts. Western blots loaded with purified SCP-2 (1–10 ng) run alongside samples from each feeding group allowed estimation of SCP-2 (μg/mg protein) in the liver homogenates (Fig. 3D). While the cholesterol-rich diet did not significantly change hepatic SCP-2 content in female versus male WT mice, SCP-2 levels were increased a respective 2.6- and 1.3-fold in female and male SCP-2-overexpressing mice compared with control-fed animals (Fig. 3A). Levels of sterol carrier protein-x (SCP-x), the only known peroxisomal branched-chain 3-ketoacyl-CoA thiolase involved in the oxidation of the branched-side chain of cholesterol (reviewed in Ref. 18), were also determined. Quantitative analysis of multiple Western blots (normalized to the housekeeping gene GAPDH) revealed hepatic levels of SCP-x were significantly lower in control-fed female versus male WT mice (Fig. 3B). Furthermore, SCP-2 overexpression increased SCP-x levels 2.2-fold in female mice and concomitantly decreased SCP-x expression 44% in male mice. The cholesterol-rich diet significantly reduced SCP-x content in all groups examined, with the largest reduction in female SCP-2-overexpressing mice (Fig. 3B).

Effect of SCP-2 overexpression and cholesterol-rich diet on whole-body phenotype

WT and SCP-2-overexpressing male and female mice were placed on a control or a high-cholesterol diet (1.25% cholesterol), followed by measurement of food consumption and body weight as described in Materials and Methods. Mice in each group consumed similar amounts of food for both the control and cholesterol-rich diet (data not shown), but weight gain was dependent on diet and SCP-2 overexpression in a sex-dependent manner, where female and male WT mice gained a respective 5.8% and 8.8% increase in body weight on the cholesterol-rich diet (**Fig. 4A, B**). SCP-2 overexpression did not further exacerbate the weight gain in males (8.8% vs. 9.2%), yet SCP-2-overexpressing females were visually larger than their wild-type counterparts and the percentage change in weight was significantly increased from 5.8% to 7.9% on the cholesterol-rich diet (Fig. 4A).

Effect of SCP-2 overexpression and cholesterol-rich diet on liver weight

Livers of control-fed WT male mice were significantly larger than those of WT female mice, regardless whether expressed as liver weight (Fig. 4D vs. C) or as liver weight/body weight (Fig. 4F vs. E). Although SCP-2 overexpression did not significantly alter the absolute liver weight in either control-fed female (Fig. 4C) or male (Fig. 4D) mice, nevertheless, SCP-2 overexpression decreased liver weight/body weight 31% in male (Fig. 4F) but not female (Fig. 4E) control-fed mice. The cholesterol-rich diet increased liver weight in both female (Fig. 4C) and male (Fig. 4D) mice, but when expressed as liver weight/body weight, only in female mice (Fig. 4E). SCP-2 overexpression did not significantly affect liver weight or liver weight/body weight in cholesterol-fed female (Figs. 3E, 4C) or male (Fig. 4D, F) mice.

Effect of SCP-2 overexpression and cholesterol-rich diet on liver morphology

Although livers from female and male WT and SCP-2 overexpression mice on control diet appeared grossly normal, after 28 days on the cholesterol-rich diet, livers of all mouse groups appeared pale and mottled, especially in the SCP-2-overexpressing female mice. Since this morphology was indicative of increased hepatic lipid accumulation, liver sections in each group were stained with osmium tetroxide and potassium dichromate (a stain for neutral lipids) as described in Materials and Methods. Cholesterol-rich diet resulted in substantially increased staining (**Fig. 5B**, D, F, H vs. Fig. 5A, C, E, G), indicative of increased lipid content. SCP-2 overexpression further increased staining of hepatic lipids, especially in the female mice (Fig. 5F vs. G). When the percentage area of hepatic lipid droplets was quantitatively analyzed for all mice in each feeding group, a significant 15- and 1.9-fold increase in hepatic lipids was observed in the cholesterol-rich diet fed female SCP-2 overexpression liver samples compared with control-fed SCP-2 over-

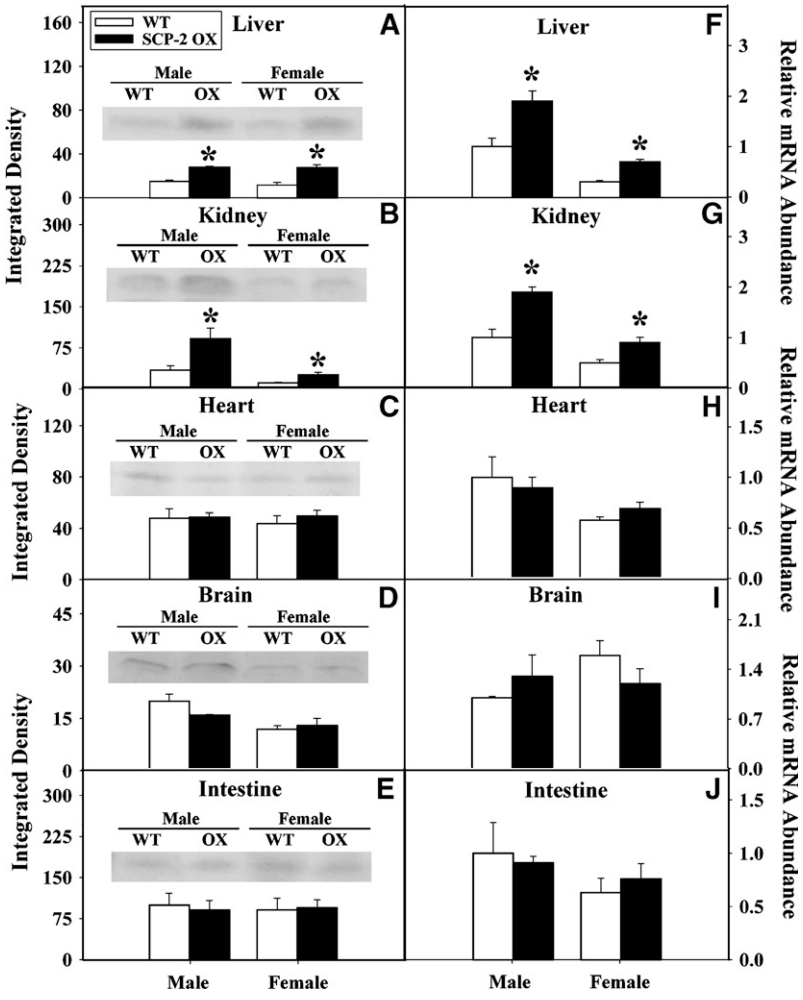

Fig. 2. Relative protein and mRNA abundance of SCP-2 expression in liver, kidney, heart, brain, and intestine. Western blot (A–E) and real-time PCR (panels F–J) analysis were used to determine protein and mRNA levels of SCP-2 in control-fed male and female WT (open bars) and SCP-2 overexpression (closed bars) mice in the following tissues: liver (A and F), kidney (B and G), heart (C and H), brain (D and I), and intestine (E and J). Representative Western blots showing SCP-2 expression levels were shown in the following tissues: liver (inset, A), kidney (inset, B), heart (inset, C), brain (inset, D), and intestine (inset, E) with the GAPDH signal used as a loading control to normalize protein expression. Values represent means ± SEM (n = 3–5). * Indicates $P < 0.02$ versus WT tissues.

expressors and cholesterol-fed WT controls (**Fig. 6A**), respectively. Similarly, hepatic lipids increased severalfold when cholesterol-rich male SCP-2 overexpression and WT liver samples were compared with their control-fed counterparts (Fig. 6B).

Effect of SCP-2 overexpression and cholesterol-rich diet on hepatic lipid composition

To establish whether a cholesterol-rich diet and SCP-2 overexpression selectively altered lipids primarily distributed into intracellular storage lipids (cholesteryl ester + triacylglycerol) or membranes (phospholipid + cholesterol), total lipids were extracted and analyzed as described in Materials and Methods. Total hepatic lipid content (intracellular storage lipids + membrane lipids) of control-fed female and male mice did not differ significantly, regardless of genotype (totals not shown). However, when placed on the cholesterol-rich diet, total hepatic lipid content in female WT and SCP-2-overexpressing mice significantly increased 4- and 4.8-fold, respectively. The cholesterol-rich diet also increased total lipid content in male WT and SCP-2-overexpressing mice by 1.9- and 3.0-fold, respectively (**Table 1**). Thus, the hepatic total lipid content of male mice was less affected by dietary cholesterol than that of females. However, SCP-2 overexpression potentiated the effect of high cholesterol diet on hepatic total lipid accumulation more in males (1.8-fold) than females (1.2-fold).

The increase in total hepatic lipids was primarily due to increased content of intracellular storage lipids (triacylglycerol + cholesteryl ester). The cholesterol-rich diet increased the content of intracellular storage lipids in female WT and even more so in SCP-2-overexpressing mice (Fig. 6C). Although the cholesterol-rich diet also increased liver intracellular storage lipids in male WT, and more so in SCP-2 overexpressing mice (Fig. 6D), this effect was less prominent than observed with female mice. The cholesterol-rich diet also increased liver content of membrane lipids (phospholipids + cholesterol). The cholesterol-rich diet increased the membrane lipid content in cholesterol-fed WT and SCP-2-overexpressing mice, but again, more so with female (Fig. 6E) than male (Fig. 6F) mice.

Effect of SCP-2 overexpression and cholesterol-rich diet on individual hepatic lipid classes

Cholesteryl esters and triacylglycerols comprise the two major lipid classes in intracellular storage lipids. In general, livers of control-fed male mice had higher levels of

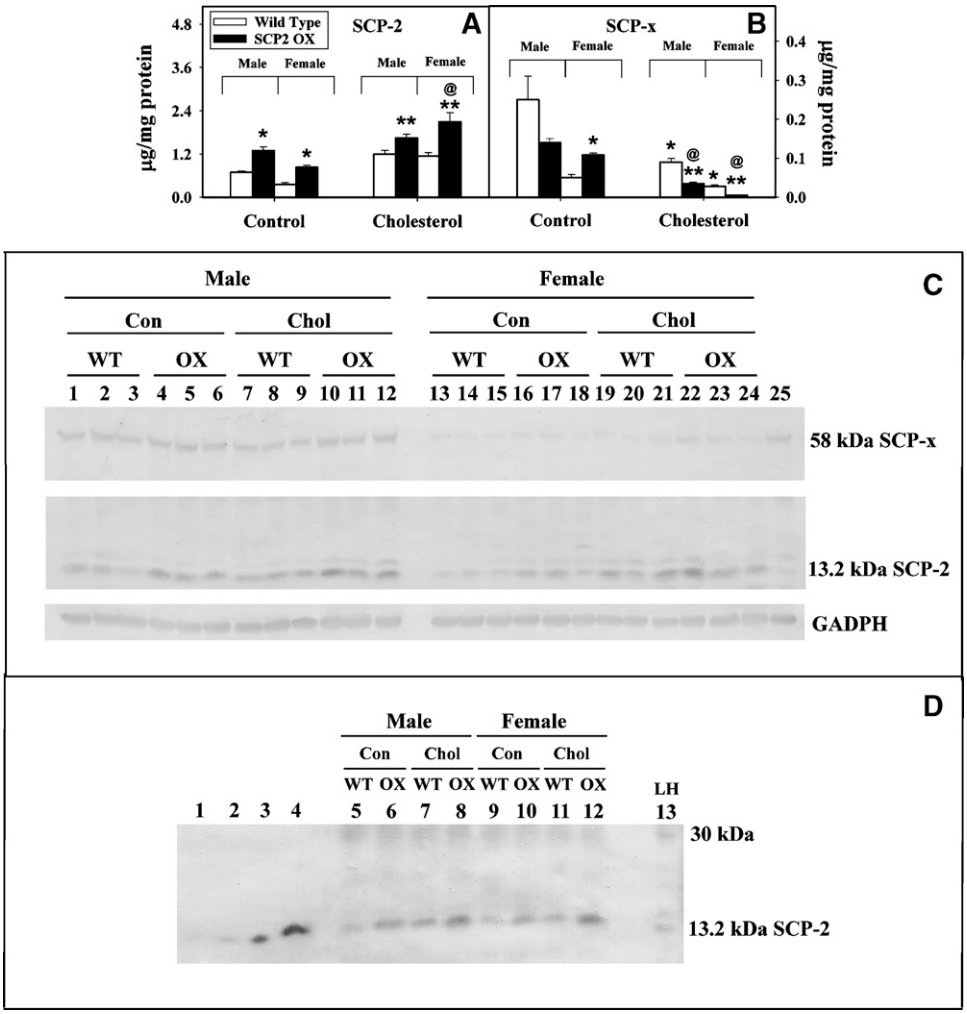

Fig. 3. Effect of SCP-2 overexpression and cholesterol-rich diet on hepatic levels of SCP-2 and SCP-x. Western blot analysis was performed to determine SCP-2 (A) and SCP-x (B) levels in male and female WT (open bar) and SCP-2-overexpressing (closed bar) mice on control and cholesterol-rich diets as described in Materials and Methods. Values represent means ± SEM (n = 3) from quantitative analysis of Western blots probed with affinity-purified antibodies against SCP-x and SCP2 (C), where the GAPDH signal was used as a loading control to normalize protein expression. * Indicates $P < 0.02$ versus WT mice on control diet; ** indicates $P < 0.01$ versus SCP-2 overexpression mice on control diet; and the "at" symbol (@) indicates $P < 0.01$ versus WT mice on cholesterol-rich diet. A representative Western blot loaded with purified SCP-2 (1–10 ng) run alongside liver homogenates from each feeding group (D) allowed estimation of SCP-2 (µg/mg protein) in each sample. OX, SCP-2 overexpressor; Con, control diet; Chol, cholesterol-rich diet; LH, liver homogenate standard.

cholesteryl ester and triacylglycerol than control-fed female mice (Table 1). However, while the cholesterol-rich diet increased cholesteryl ester and triacylglycerol content in both male and female mice, the effect was less in male than that observed with the female mice, whether in WT and SCP-2-overexpressing mice. The cholesterol-rich diet increased hepatic free cholesterol 6.7- and 4.8-fold in WT female and male mice, respectively (Table 1), and markedly increased the percentage of esterified cholesterol in WT females but not males. SCP-2 overexpression increased the unesterified and esterified cholesterol content in both cholesterol-fed female and male mice (Table 1). While hepatic triacylglycerol content was also significantly increased in the cholesterol-fed animals, SCP-2 overexpression potentiated this effect only in male mice (Table 1). With regard to phospholipid levels, there was no significant effect of sex or SCP-2 expression in control-fed mice, but cholesterol-rich diet increased hepatic phospholipid content in all groups examined, especially in females (Table 1).

Effect of SCP-2 overexpression and cholesterol-rich diet on serum levels of total cholesterol, phospholipid, and bile acids

Serum lipid levels were determined in WT and SCP-2 overexpression mice on control and cholesterol-rich diet as described in Materials and Methods. Cholesterol and bile acid content in control and cholesterol-fed WT mice were not significantly different regardless of sex (**Table 2**). Phospholipid levels were decreased in male, but not female, cholesterol-fed WT mice. The effect of SCP-2 overexpression

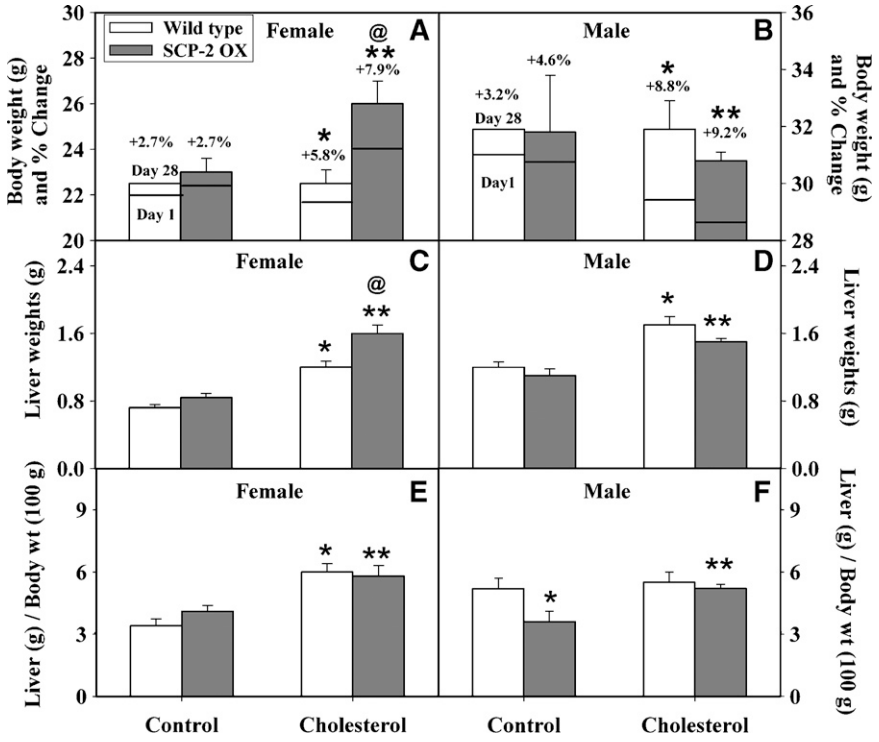

Fig. 4. Body weight, percentage change in body weight, liver weight, and liver/body weight. Body weight (g) and percentage change in body weight (A, B), liver weight (C, D), and liver/body weight (E, F) were measured in female (A, C, E) and male (B, D, F) WT (open bars) and SCP-2-overexpressing (closed bars) mice on control and cholesterol-rich diets at days 1 and 28 of the feeding study. Values represent means ± SEM (n = 5–7). * Indicates $P < 0.02$ versus WT mice on control diet; ** indicates $P < 0.01$ versus SCP-2 overexpression mice on control diet; and the "at" symbol (@) indicates $P < 0.01$ versus WT mice on cholesterol-rich diet.

was to increase lipid levels in both male and female mice. However, in response to the cholesterol diet, SCP-2 overexpression decreased total cholesterol, phospholipid, and bile acid levels (Table 2).

Effect of SCP-2 overexpression and cholesterol-rich diet on serum lipoprotein profiles

Lipoprotein profiles of serum obtained from male and female WT and SCP-2-overexpressing mice fed a control and cholesterol-rich diet demonstrated that the HDL fraction contained the most cholesterol (**Fig. 7**), with lower levels observed in the LDL fraction. Little to no VLDL was observed, most likely because the animals were fasted overnight. From the lipoprotein profiles (Fig. 7A, B) and quantitative analysis of cholesterol levels (Fig. 7C, D), a unique pattern of cholesterol distribution was observed for each lipoprotein fraction. In male (data not shown) and female (Fig. 7A) WT mice, levels of HDL cholesterol were lower in control-fed mice compared with cholesterol-fed animals. In contrast, in SCP-2 overexpression mice (Fig. 7B), HDL cholesterol levels were lower in the cholesterol-fed mice (Fig. 7C). A similar trend was not observed with LDL-cholesterol (Fig. 7D) where in both WT and SCP-2-overexpressing cholesterol-fed mice an increase in LDL-cholesterol was observed. Taken together, these results were consistent with a role for SCP-2 in the regulation of lipoprotein cholesterol metabolism.

Effect of SCP-2 overexpression and cholesterol-rich diet on biliary conconcentrations of total cholesterol, phospholipid, and bile salts

Lipid levels in the gall bladder were determined in WT and SCP-2 overexpression mice on control and cholesterol-rich diets. While the effects of SCP-2 overexpression on lipid content in control-fed mice were minimal, regardless of sex (**Table 3**), the cholesterol-rich diet increased levels of cholesterol, phospholipid, and bile acids in male and female WT mice and increased cholesterol and phospholipid content in SCP-2 overexpression mice (Table 3). Bile acid concentrations increased in response to cholesterol in WT female mice and also in control-fed SCP-2 overexpression female mice.

Effect of SCP-2 overexpression and cholesterol-rich diet on total bile acid content

Bile acid content in liver, serum, and gall bladder was determined in WT and SCP-2 overexpression mice on control and cholesterol-rich diet. Levels of hepatic bile salts of control-fed SCP-2 overexpression male, but not female, mice were significantly increased versus their WT counterparts (**Table 4**). The cholesterol-rich diet increased hepatic bile salt level in both male and female WT mice. The effect of SCP-2 overexpression in female control-fed mice was minimal but increased 1.7-fold in male mice. However, SCP-2 overexpression in response to cholesterol-rich diet

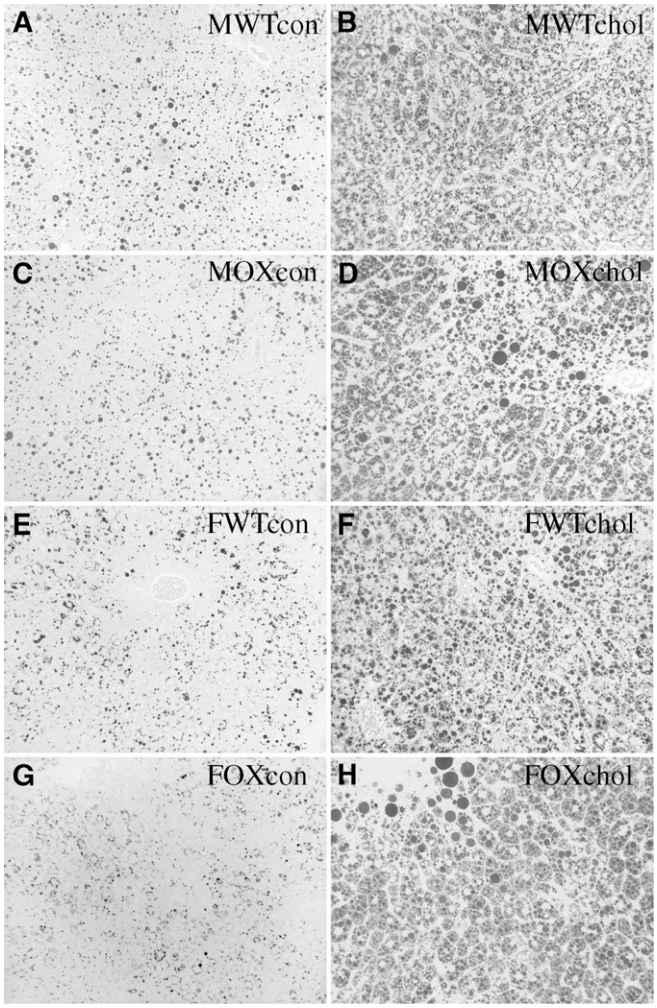

Fig. 5. Hepatic lipid accumulation in liver sections from male and female SCP-2 transgenic mice fed a cholesterol-rich diet. Liver thin sections from male (A–D) and female (E–H) WT (A, B, E, F) and SCP-2-overexpressing (C, D, G, H) mice on control (A, C, E, G) and cholesterol-rich (B, D, F, H) diets were stained with osmium tetroxide and potassium dichromate for image analysis of lipids by light microscopy as described in Materials and Methods. MWTcon, male WT mice on control diet; MWTchol, male WT mice on cholesterol-rich diet; MOXcon, male SCP-2-overexpressing mice on control diet; MOXchol, male SCP-2-overexpressing mice on cholesterol-rich diet; FWTcon, female WT mice on control diet; FWTchol, female WT mice on cholesterol-rich diet; FOXcon, female SCP-2-overexpressing mice on control diet; FOXchol, female SCP-2-overexpressing mice on cholesterol-rich diet.

regardless of sex was to decrease hepatic bile salt content in male and female mice when compared with control or cholesterol-fed animals (Table 4). Similar decreases were observed in serum but not biliary bile acid content when compared with control-fed mice. Overall, since the major concentration of bile acids is located in the gall bladder, trends in the total bile acid content reflected trends observed with biliary bile salts that were minimal.

Effect of SCP-2 overexpression and cholesterol-rich diet on hepatic proteins involved in cholesterol uptake: LDL-receptor

In order to begin to resolve the mechanism(s) whereby SCP-2 potentiated hepatic cholesterol accumulation, especially in mice fed a cholesterol-rich diet, the effect of SCP-2 overexpression and cholesterol-rich diet on the levels of hepatic proteins involved in cholesterol metabolism were examined. A major portion of cholesterol transported to the liver enters hepatocytes through the LDL-receptor pathway (40). Hepatic LDL-receptor levels were 1.5-fold higher in male than female control-fed mice (**Fig. 8A**). SCP-2 overexpression increased hepatic LDL-receptor levels 1.5- and 1.6-fold in male and female control-fed mice, respectively. Cholesterol-rich diet also increased levels of LDL-receptor in female 1.4-fold, but not male mice (Fig. 8A). SCP-2 overexpression did not further increase LDL-receptor in cholesterol-fed female mice, but decreased that in cholesterol-fed male mice (Fig. 8A). In short, the effect of SCP-2 overexpression on the LDL-receptor, a major receptor involved in hepatic cholesterol uptake, was to increase expression nearly 1.6-fold in control fed mice, regardless of gender, while the cholesterol-rich diet negated this effect.

Effect of SCP-2 overexpression and cholesterol-rich diet on hepatic proteins involved in reverse cholesterol uptake: HDL-receptor SR-B1

Hepatic HDL-mediated uptake/efflux of cholesterol is mediated through SR-B1 and several proteins that regulate SR-B1 level and localization at the plasma membrane, including PDZK1 and MAP-17 (7). SR-B1 was significantly lower in control-fed female than in male WT mice (Fig. 8B). SCP-2 overexpression resulted in a 1.9-fold increase of SR-B1 expression in control-fed female mice with no change observed with the male mice. In wild-type mice, the cholesterol-rich diet differentially altered SR-B1expression in a sex-dependent manner: increased SR-B1 in females and reduced SR-B1 in males. In contrast, cholesterol-rich diet reduced SR-B1 expression in both sexes of SCP-2 overexpression mice when compared with the control-fed counterparts (Fig. 8B).

PDZK-1 is a scaffolding protein present at both basolateral and apical (canalicular) membranes where it binds the cytoplasmic C terminus of SR-B1 and targets SR-B1 to the plasma membrane (7). The level of PDZK-1 was significantly lower in control-fed female than in male WT mice—consistent with the lower level of SR-B1 in females (Fig. 8C). SCP-2 overexpression resulted in a 3.6-fold increase in PDZK-1 expression in control-fed female mice but not in male mice—again consistent with the higher level of SR-B1 in females. While the cholesterol-rich diet increased expression of PDZK-1 in female WT and SCP-2 overexpression mice, this increase correlated with increased SR-B1 only in the control-fed females, suggesting contributions from additional factor(s) existing under conditions of cholesterol-rich diet (Fig. 8C). The cholesterol-rich diet did not alter expression of PDZK-1 in male WT and SCP-2 overexpression mice, not correlating with the observed decrease in SR-B1 level, but suggesting contributions from additional factor(s) under conditions of cholesterol-rich diet (Fig. 8C).

MAP-17 is thought to be a canalicular protein where it normally interacts with PDZK-1 and regulates its targeting to the plasma membrane (7, 41). In contrast, when MAP-17

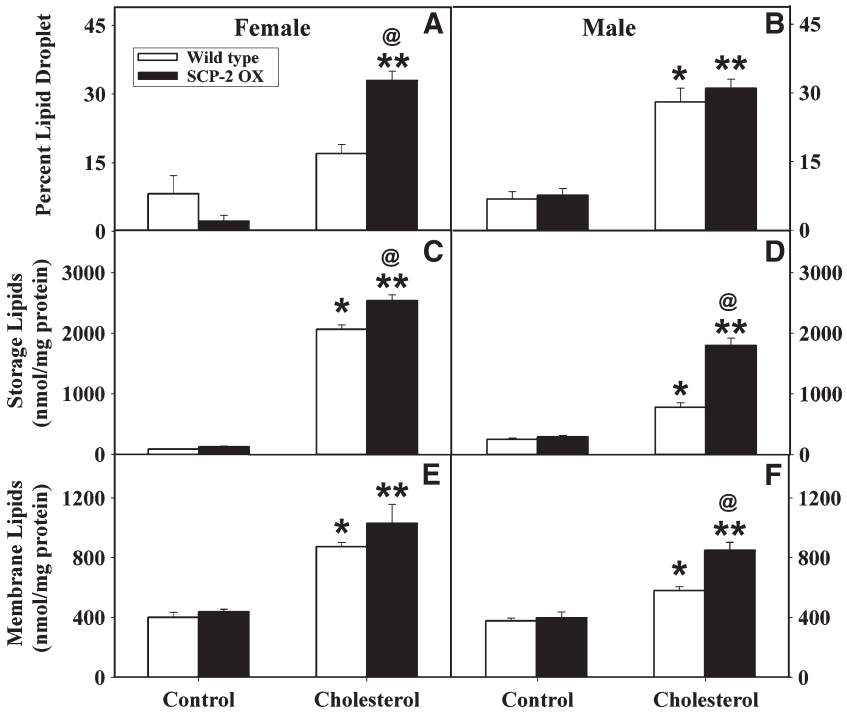

Fig. 6. Percentage lipid droplet, storage lipids, and membrane lipids in liver. The percentage lipid droplet (A, B), storage lipid (C, D), and membrane lipid (E, F) content in liver sections from female (A, C, E) and male (B, D, F) WT (open bars) and SCP-2-overexpressing (closed bars) mice on control and cholesterol-rich diet was determined as described in Materials and Methods. Values represent means ± SEM (n = 3). * Indicates $P < 0.05$ versus WT mice on control diet; ** indicates $P < 0.05$ versus SCP-2 overexpression mice on control diet; and the "at" symbol (@) indicates $P < 0.05$ versus WT mice on cholesterol-rich diet.

levels are increased above a physiological threshold, MAP-17 stimulates PDZK1 posttranslational degradation and decreases SR-B1 (7, 41). Levels of MAP-17 were significantly lower in control-fed female than in male WT mice, but levels of PDZK1 and SR-B1 were not higher in females—consistent with the normal physiological conditions (Fig. 8D). Likewise, SCP-2 overexpression in the physiological range increased MAP-17 expression by 9.4-fold in control-fed female, but not in male, mice and increased, rather than decreased, levels of PDZK1 and SR-B1. Cholesterol-rich diet alone increased the expression of MAP-17 in both male and female WT mice, but SR-B1 decreased only in male mice (Fig. 8D).

TABLE 1. Effect of SCP-2 overexpression and cholesterol-rich diet on hepatic lipid levels

	WT		SCP-2 Overexpressor	
Lipid	Control	Cholesterol	Control	Cholesterol
		Female Mice		
Cholesteryl ester	40 ± 8	1,422 ± 90*	82 ± 3*	2,034 ± 89**@
Triacylglycerol	46 ± 9	645 ± 69*	43 ± 14	503 ± 34**
Free fatty acids	449 ± 88	794 ± 19*	379 ± 105	988 ± 45**@
Cholesterol	29 ± 4	195 ± 11*	56 ± 4*	269 ± 24**@
Phospholipid	373 ± 33	679 ± 27*	381 ± 18	761 ± 125**
Total lipid	937 ± 94	3735 ± 118*	941 ± 107	4,555 ± 165**@
Total cholesterol	69 ± 9	1,617 ± 91*	138 ± 5*	2,303 ± 92**@
C/P ratio	0.08 ± 0.01	0.3 ± 0.02*	0.15 ± 0.01*	0.35 ± 0.07**
		Male Mice		
Cholesteryl ester	83 ± 18	508 ± 64*	127 ± 14	903 ± 69**@
Triacylglycerol	168 ± 13	273 ± 40*	177 ± 19	896 ± 103**@
Free fatty acids	440 ± 24	698 ± 61*	454 ± 36	855 ± 43**@
Cholesterol	28 ± 7	135 ± 9*	48 ± 5*	174 ± 7**@
Phospholipid	350 ± 17	446 ± 23*	350 ± 40	676 ± 53***@
Total lipid	1,069 ± 38	2,060 ± 100*	1,156 ± 67	3504 ± 142**@
Total cholesterol	111 ± 19	643 ± 65*	175 ± 15*	1,077 ± 69**@
C/P ratio	0.08 ± 0.02	0.3 ± 0.03*	0.14 ± 0.02	0.26 ± 0.02**

Values represent means (nmol/mg protein) ± SE, n = 3–8. * Indicates $P < 0.05$ compared with WT mice on the control diet. ** Indicates $P < 0.03$ compared with SCP-2-overexpressing mice on the control diet. The "at" symbol (@) indicates $P < 0.02$ compared with mice on the cholesterol-rich diet. C/P ratio indicates cholesterol-to-phospholipid ratio.

TABLE 2. Effect of SCP-2 overexpression and cholesterol-rich diet on serum levels of total cholesterol, phospholipids, and bile acids

	WT		SCP-2 Overexpressor	
Lipid	Control	Cholesterol	Control	Cholesterol
		Female Mice		
Total cholesterol	3.5 ± 0.5	2.3 ± 0.2	4.3 ± 0.4	3.3 ± 0.2@
Phospholipid	2.3 ± 0.3	2.2 ± 0.3	3.7 ± 0.2*	2.1 ± 0.2**
Bile acid	22 ± 4	22 ± 3	40 ± 0.6*	27 ± 5**
		Male Mice		
Total cholesterol	5.1 ± 0.2	5.0 ± 0.3	5.6 ± 0.1	5.3 ± 0.4
Phospholipid	4.5 ± 0.1	3.7 ± 0.2*	4.7 ± 0.1	3.9 ± 0.2**
Bile acid	23 ± 3	25 ± 4	41 ± 6*	20 ± 2**

Concentrations of serum total cholesterol (mmol/L), phospholipids (mmol/L), and bile acid (μmol/L) were determined as described in Materials and Methods. Values represent means ± SE, n = 3–8. * Indicates $P < 0.04$ compared with WT mice on the control diet. ** Indicates $P < 0.05$ compared with SCP-2-overexpressing mice on the control diet. The "at" symbol (@) indicates $P < 0.01$ compared with mice on the cholesterol-rich diet.

In contrast, cholesterol-rich diet increased hepatic MAP-17 in both male and female SCP-2-overexpressing mice, while concomitantly decreasing SR-B1 (Fig. 8D).

Effect of SCP-2 overexpression and cholesterol-rich diet on hepatic proteins that bind/transport cholesterol through the cytoplasm (L-FABP and caveolin-1)

Besides SCP-2, there are two other key intracellular proteins that bind and transport cholesterol from the plasma membrane to intracellular sites: L-FABP and caveolin-1 (reviewed in Refs. 8 and 18). L-FABP expression in control-fed female WT and SCP-2-overexpressing mice was 3.1- and 1.3-fold lower, respectively, than in the corresponding male counterparts (Fig. 8H). SCP-2 overexpression had no effect on L-FABP content in control-fed males but increased levels 2.3-fold in females. However, overexpression of SCP-2 significantly decreased L-FABP content in male but not female cholesterol-fed mice compared with WT cholesterol-fed counterparts (Fig. 8H).

Caveolin-1 levels were not dependent on sex or SCP-2 overexpression in control-fed mice (Fig. 8G). However, cholesterol-rich diet significantly affected caveolin-1 in SCP-2-overexpressing female mice (Fig. 8G), which exhibited reduced caveolin-1 levels.

Effect of SCP-2 overexpression and cholesterol-rich diet on hepatic proteins involved in cholesterol synthesis and esterification (ACAT2 and HMG-CoA reductase)

ACAT mediates esterification of plasma membrane-derived cholesterol in the endoplasmic reticulum of cells, and ACAT2 is the major isoform in liver (reviewed in Refs. 36 and 37). ACAT2 levels were not dependent on sex in control-fed mice but were increased 1.4-fold in SCP-2-overexpressing males but not females (**Fig. 9A**). Cholesterol-rich diet did not significantly affect ACAT2 level in WT mice but decreased that in SCP-2-overexpressing mice versus the respective control-fed mice (Fig. 9A). Thus, ACAT2 levels were in the following order: cholesterol-fed SCP-2 overexpressor males < control-fed WT females < cholesterol-fed WT males and SCP-2 overexpressor females < cholesterol-fed WT females < control-fed WT males and SCP-2 overexpressor females < control-fed SCP-2 overexpressor males.

Levels of HMG-CoA reductase, a key enzyme regulating cholesterol synthesis, were determined by real-time PCR as described in Materials and Methods. Neither sex nor SCP overexpression affected the relative mRNA abundance of HMG-CoA reductase in control-fed male and female mice (**Fig. 10D**). However, the cholesterol-rich diet significantly decreased levels in WT female but not male mice. In addition, SCP-2 overexpression and cholesterol-rich diet together further decreased HMG-CoA reductase expression with significantly lower levels observed in both male and female mice compared with control-fed mice (Fig. 10D).

Effect of SCP-2 overexpression and cholesterol-rich diet on key enzymes involved in cholesterol oxidation to and transport of bile acids (CYP7A1, CYP27A1, 3αHSD, Oatp1a1, Oatp1a4, and Ntcp)

SCP-2 overexpression significantly increased hepatic, serum, and biliary concentrations of bile salts, yet the effect of SCP-2 overexpression in response to the cholesterol-rich diet was to decrease levels (Table 4). Thus, it was important to determine if these results were due to altered regulation of proteins involved in cholesterol oxidation to bile acids (CYP7A1 and CYP27A1) and/or transport of bile acids (3α-HSD, Oatp1a1, Oatp1a4, and Ntcp).

CYP7A1 (involved in the rate-limiting step of bile acid synthesis) and CYP27A1 are two key enzymes in the hepatic bile acid synthetic pathway. Protein levels for both CYP7A1 (Fig. 9C) and CYP27A1 (Fig. 9D) and mRNA levels for CYP7A1 (Fig. 10C) were not dependent on sex or SCP-2 overexpression in control-fed mice. However, the cholesterol-rich diet significantly increased CYP7A1 levels in male and female WT and SCP-2-overexpressing mice (Figs. 9C, 10C). In contrast, levels of CYP27A1 were not affected by the cholesterol-rich diet in male or female WT mice, but a respective 1.6- and 1.5-fold decrease in expression was observed with male and female SCP-2-overexpressing mice when compared with their control-fed counterparts (Fig. 9D).

Levels of 3α-HSD (Fig. 9B), Oatp1a1 (Fig. 10G), Oatp1a4 (Fig. 10H), and Ntcp (Fig. 10E) proteins involved in bile acid binding/transport through the cytoplasm or across the plasma membrane (reviewed in Refs. 36, 37, 42, and 43), were not dependent on sex in control-fed mice. In addition, SCP-2 overexpression had no effect in control-fed male or female mice, except 3α-HSD increased 2.6-fold in control-fed female mice (Fig. 9B). The cholesterol-rich diet increased expression of 3α-HSD (Fig. 9B) and Ntcp (Fig. 10E) in female WT and SCP-2 overexpression mice, while levels of Oatp1a1 and Oatp1a4 were decreased in female SCP-2 overexpressors (Fig. 10G, H).

Effect of SCP-2 overexpression and cholesterol-rich diet on key nuclear receptors involved in cholesterol and bile acid synthesis (SREBP-2, LXR-α, and SHP)

Several nuclear receptors regulate transcription of numerous genes involved in cholesterol uptake/metabolism: SREBP-2 downregulates transcription of HMG-CoA reductase;

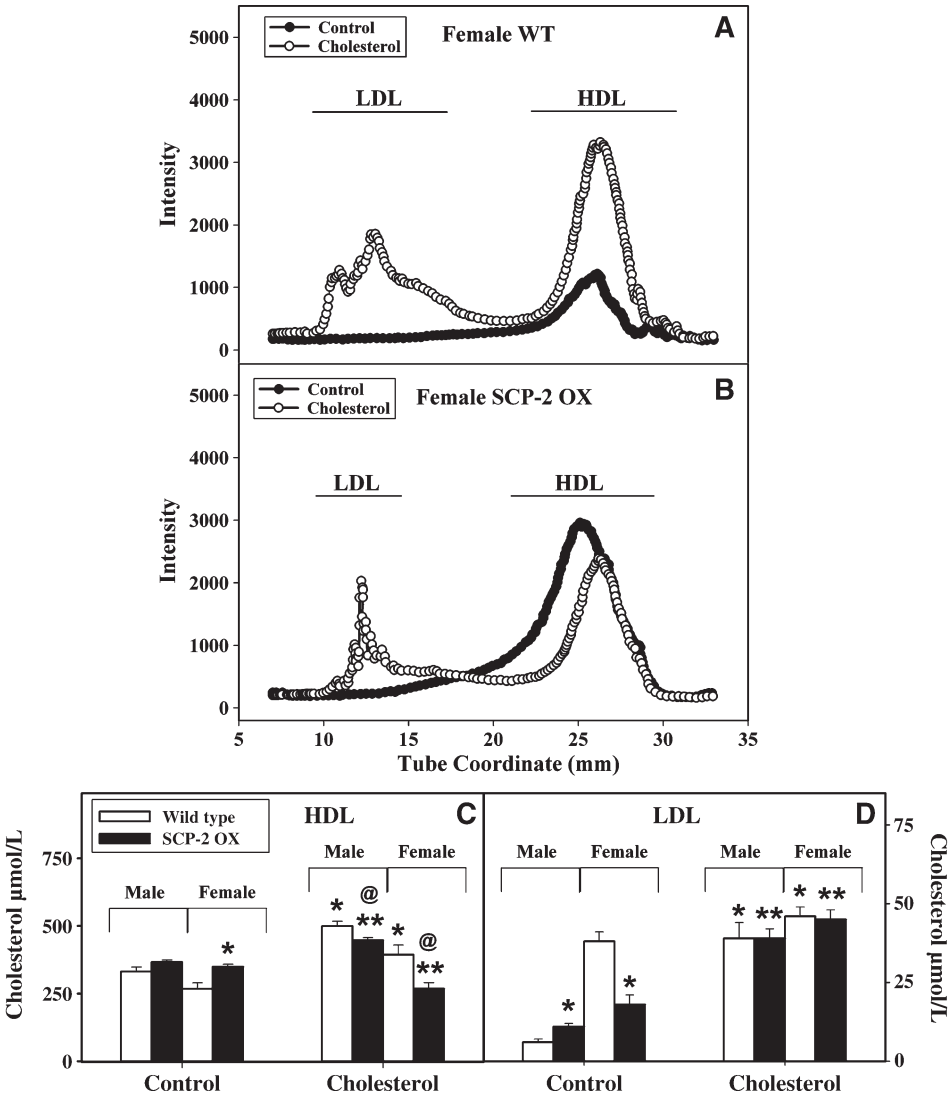

Fig. 7. Effect of SCP-2 overexpression and cholesterol-rich diet on serum lipoprotein profiles. Serum lipoprotein profiles from female WT (A) and SCP-2-overexpressing (B) mice were determined, and levels of cholesterol (μmol/L) in the LDL (C) and HDL (D) fractions from male and female WT (open bars) and SCP-2-overexpressing (closed bars) mice were quantitated using a Wako kit as described in Materials and Methods. Values represent means ± SEM (n = 3). * Indicates $P < 0.05$ versus WT mice on control diet; ** indicates $P < 0.05$ versus SCP-2 overexpression mice on control diet; and the "at" symbol (@) indicates $P < 0.05$ versus WT mice on cholesterol-rich diet.

and LXR-α and SHP are positive and negative transcriptional regulators, respectively, of the rate-limiting enzyme in bile acid synthesis (CYP7A1) and other enzymes of bile acid synthesis (reviewed in Refs. 36 and 37). Therefore, it was important to determine whether the hepatic levels of these proteins were associated with hepatic cholesteryl ester and cholesterol accumulation induced by SCP-2 overexpression, especially in mice fed a cholesterol-rich diet. SREBP-2, regulated by cholesterol and coregulated by dietary fat, exists in two forms, a 125 kDa inactive membrane-associated form and a 68 kDa active nuclear form (reviewed in Refs. 36 and 37). While hepatic levels of the inactive form did not change within the study groups (data not shown), levels of the nuclear form of SREBP-2 were significantly lower in control-fed female than in male WT mice (Fig. 10F). In addition, the nuclear form of SREBP-2 was not SCP-2 expression dependent in control-fed female or male mice, and the cholesterol-rich diet did not increase expression in WT mice. However, SCP-2 overexpression increased SREBP-2 in cholesterol-fed female mice, a result consistent with downregulation of HMG-CoA reductase (Fig. 10D).

Levels of the nuclear hormone receptors LXR-α (a positive regulator of cholesterol/bile acid synthesis) and SHP (a negative regulator) were not dependent on sex in control-fed mice (Fig. 9E, F). However, SCP-2 overexpression decreased LXR-α and SHP in control-fed female mice slightly, with no similar affects observed in male mice. The cholesterol-rich diet increased levels of LXR-α 2.6- and 5.8-fold in female WT and SCP-2 overexpression mice, respectively (Fig. 9E). Concomitantly, levels of SHP decreased 2.1-fold in female cholesterol-fed SCP-2 overexpression mice, while male mice were not similarly affected (Fig. 9F).

TABLE 3. Effect of SCP-2 overexpression and cholesterol-rich diet on biliary concentrations of total cholesterol, phospholipids, and bile acids

Lipid	WT		SCP-2 Overexpressor	
	Control	Cholesterol	Control	Cholesterol
			Female Mice	
Total cholesterol	1.6 ± 0.2	6.5 ± 0.2*	1.6 ± 0.3	4.4 ± 0.2**,@
Phospholipid	17.2 ± 0.9	30 ± 1*	16.0 ± 0.8	25 ± 6
Bile acid	184 ± 16	288 ± 15*	310 ± 13*	294 ± 15
			Male Mice	
Total cholesterol	1.6 ± 0.2	3.4 ± 0.3*	1.2 ± 0.1	4.7 ± 0.2**,@
Phospholipid	18.1 ± 0.8	14.5 ± 0.6*	17.3 ± 0.8	22 ± 1**,@
Bile acid	293 ± 15	315 ± 16	270 ± 7	298 ± 11

Concentrations of total cholesterol (mmol/L), phospholipids (mmol/L), and bile acids (mmol/L) were determined as described in Materials and Methods. Values represent means ± SE, n = 3–8. * Indicates $P < 0.002$ compared with WT mice on the control diet. ** Indicates $P < 0.003$ compared with SCP-2-overexpressing mice on the control diet. The "at" symbol (@) indicates $P < 0.007$ compared with mice on the cholesterol-rich diet.

Effect of SCP-2 overexpression and cholesterol-rich diet on hepatic proteins involved in cholesterol efflux (ABCA-1, ABCG5, ABCG8, and apoA1)

Two major plasma membrane pathways facilitating cholesterol efflux from the liver use different proteins within the plasma membrane include *i*) the energy-independent scavenger receptor B1 (SR-B1), which mediates not only uptake of cholesterol from HDL but also efflux of cholesterol to HDL as discussed above; and *ii*) the ATP-requiring cassette transporters ABCA-1 (to apoA1) and ABCG-1 (to HDL) with efflux through the canalicular membrane into bile facilitated by ABCG-5 and ABCG-8 (obligate heterodimers). Liver secretes apoA1 in the blood, and the ABC transporter A1 (ABCA-1) facilitates phospholipid desorption to apoA1 followed by cholesterol desorption to form HDL (reviewed in Ref. 8). ABCA-1 levels were similar in control-fed female versus male WT mice (Fig. 8E). In contrast, ABCA-1 levels were decreased 1.8-fold by SCP-2 overexpression in control-fed male mice with no significant change observed in the female mice (Fig. 8E). The cholesterol-rich diet increased ABCA-1 levels in female WT mice and tended to increase levels in the female cholesterol-fed SCP-2-overexpressing mice (Fig. 8E). Not withstanding significant changes in levels of ABCA-1, levels of apoA1 were minimally altered by SCP-2 overexpression or cholesterol-rich diet (Fig. 8F).

Levels of canalicular transporters, including ABCG5 (Fig. 10A) and ABCG8 (Fig. 10B), were similar in male and female control-fed WT and SCP-2 overexpressors. In contrast, the cholesterol-rich diet increased levels of ABCG5 and ABCG8 in both male and female WT mice, with little further enhancement observed in the SCP-2 overexpression animals.

DISCUSSION

SCP-2 is a ubiquitous protein expressed in all mammalian tissues but at highest levels in tissues active in cholesterol metabolism, including liver, steroidogenic cells (adrenal, testis, and ovary), and intestine (reviewed in Ref. 18). Despite the discovery more than 30 years ago that SCP-2 acts as a cholesterol binding/transfer protein, resolving the physiological functions of SCP-2 remains a work in progress (reviewed in Ref. 18). Numerous studies in transfected transformed cells overexpressing SCP-2 as well as correlative studies in animals have suggested a role in cholesterol uptake, intracellular cycling, esterification, and/or efflux (9–13). However, direct demonstration of a role in cholesterol metabolism in SCP-2/SCP-x gene ablated mice was complicated by concomitant 4-fold upregulation of L-FABP, a soluble protein normally accounting for 2–5% of cytosolic protein (reviewed in Refs. 9, 10, 18, and 44). L-FABP also facilitates cholesterol uptake, trafficking from the plasma membrane to the endoplasmic reticulum for esterification, and efflux (reviewed in Refs. 36, 37, and 44). Consequently, SCP-2's full physiological significance remains unknown. In this work, transgenic mice overexpressing SCP-2 (>2-fold in liver) were created by pronuclear injection. Hepatic levels

TABLE 4. Total bile acid content (nmol) in liver, serum, and gall bladder bile in control and cholesterol-fed SCP-2-overexpressing mice

Source	WT		SCP-2 Overexpressor	
	Control	Cholesterol	Control	Cholesterol
			Female Mice	
Liver	52 ± 6	145 ± 20*	52 ± 11	42 ± 6@
Serum	4.4 ± 0.7	4.4 ± 0.9	8 ± 1*	5 ± 1
Gall bladder	3,922 ± 347	5,770 ± 309*	6,209 ± 267*	5,888 ± 136
Total	3,967 ± 340	5,881 ± 291*	6,243 ± 253*	5,915 ± 129
			Male Mice	
Liver	278 ± 28	430 ± 34*	482 ± 54*	267 ± 14**,@
Serum	4.6 ± 0.5	5.0 ± 0.8	8 ± 1*	3.9 ± 0.4**
Gall bladder	5,860 ± 300	6,300 ± 320	5,400 ± 147	5,967 ± 217
Total	6,085 ± 305	6,511 ± 311	5,679 ± 207	6,147 ± 198

Levels (nmol) of total bile acid in liver, serum, and gall bladder were determined as described in Materials and Methods. Values represent means ± SE, n = 3–8. (*) indicates $P < 0.03$ compared with WT mice on the control diet. ** Indicates $P < 0.002$ compared with SCP-2-overexpressing mice on the control diet. The "at" symbol (@) indicates $P < 0.003$ compared with mice on the cholesterol-rich diet.

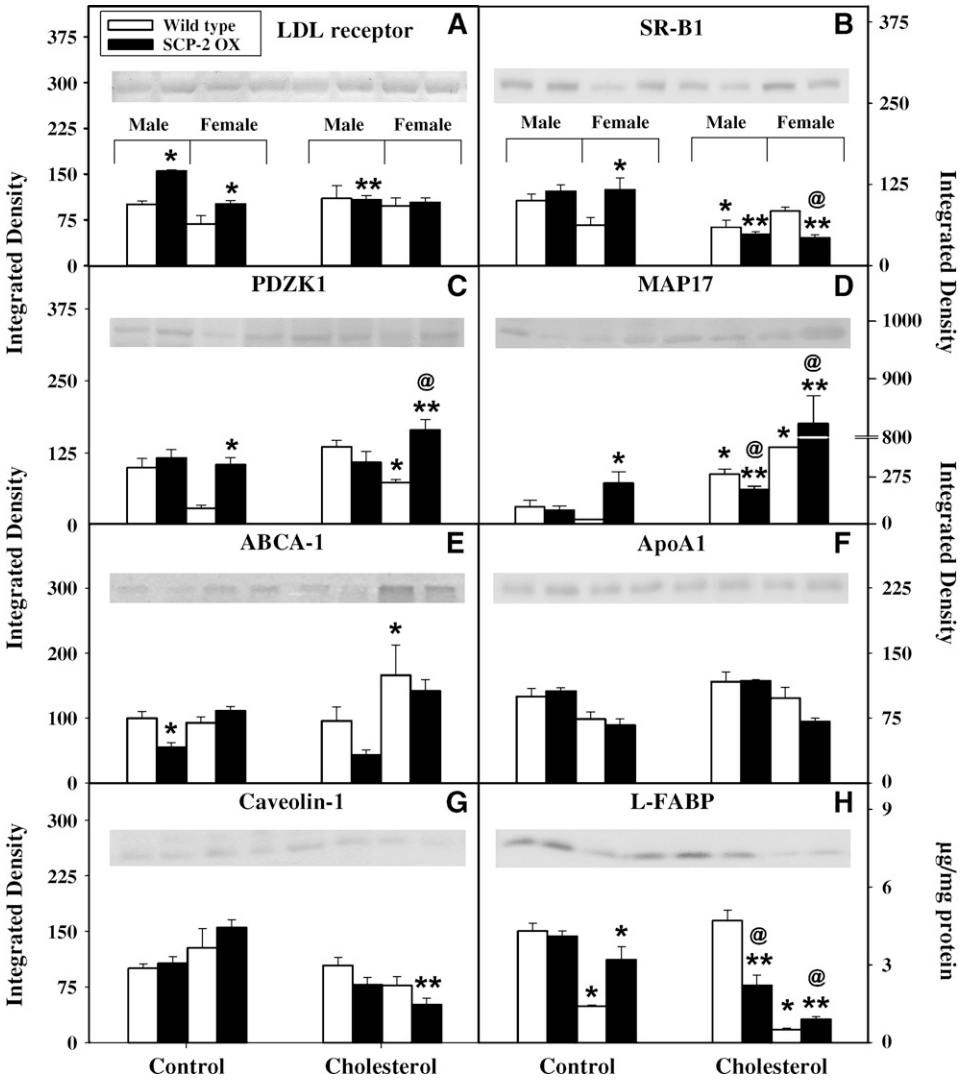

Fig. 8. Effect of SCP-2 overexpression and cholesterol-rich diet on key proteins involved in cholesterol uptake and efflux. Liver homogenates (10 μg) isolated from male and female WT (open bars) and SCP-2-overexpressing (closed bars) mice on control and cholesterol-rich diets were probed with the following affinity-purified antibodies: A, anti-LDL receptor; B, anti-SR-B1; C, anti-PDZK1; D, anti-MAP-17; E, anti-ABCA-1; F, apoA1; G, anti-caveolin-1; and H, anti-L-FABP. Expression levels were quantified as described in Materials and Methods. Insets: Representative Western blots showing relative protein expression in each mouse group. The GAPDH signal used was a loading control to normalize protein expression. Values represent means ± SEM (n = 5–7). * Indicates $P < 0.05$ versus WT mice on control diet; ** indicates $P < 0.05$ versus SCP-2-overexpressing mice on control diet; and the "at" symbol (@) indicates $P < 0.05$ versus WT mice on cholesterol-rich diet.

of the mature 13 kDa SCP-2 (derived from complete post-translational cleavage of the 15 kDa pro-SCP-2) in the SCP-2-overexpressing mice were well within the range of SCP-2 protein expression in response to normal physiological and pharmacological conditions where levels of SCP-2 can range nearly 3-fold in response to *i*) dietary branched-chain fatty acids that, acting as peroxisomal proliferator agents, upregulate SCP-2 nearly 2-fold in both male and female mice (22); and *ii*) drug-induced diabetes and cholesterol lowering drugs that downregulate SCP-2 expression 25–90% (reviewed in Ref. 18). Key physiological questions to be answered in this work include how sex, SCP-2 overexpression, and a cholesterol-rich diet affect lipids and proteins involved in hepatic cholesterol homeostasis. In order to summarize the observed findings, an illustration of cholesterol transport in a hepatocyte is provided (**Fig. 11**).

First, the cholesterol-rich diet induced whole-body weight gain, hepatic enlargement, and hepatic lipid accumulation in both female and male WT mice, while SCP-2 overexpression only slightly altered whole-body phenotype (weight gain), regardless of diet. Similarly, control-fed SCP-2/SCP-x null or SCP-x null mice also exhibited little alteration in whole body phenotype (45, 46).

Second, SCP-2 overexpression induced hepatic lipid accumulation (especially in the form of cholesteryl esters, cholesterol, and triacylglyceride) with the pattern of lipid

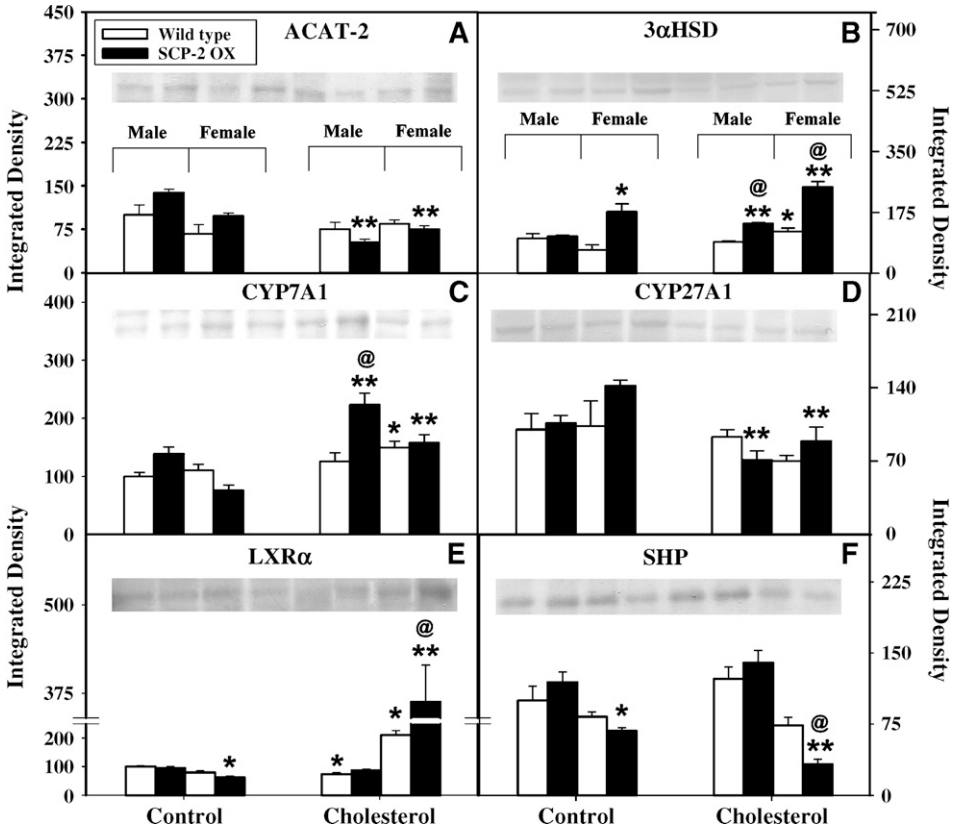

Fig. 9. Effect of SCP-2 overexpression and cholesterol-rich diet on proteins and nuclear receptors involved in cholesterol esterification, synthesis, and cholesterol oxidation to bile acids. Liver homogenates (10 μg) isolated from male and female WT (open bars) and SCP-2-overexpressing (closed bars) mice on control and cholesterol-rich diets were probed with the following affinity-purified antibodies: A, anti-ACAT2; B, anti-3α-HSD; C, anti-CYP7A1; D, anti-CYP27A1; E, anti-LXR-α; and F, anti-SHP. Expression levels were quantified as described in Materials and Methods. Insets: Representative Western blots showing relative protein expression in each mouse group. The GAPDH signal used was a loading control to normalize protein expression. Values represent means ± SEM (n = 5–7). * Indicates $P < 0.05$ versus WT mice on control diet; ** indicates $P < 0.05$ versus SCP-2 overexpressing mice on control diet; and the "at" symbol (@) indicates $P < 0.05$ versus WT mice on cholesterol-rich diet.

accumulation dependent on sex and exacerbated by cholesterol-rich diet. While both female and male SCP-overexpressing mice exhibited elevated hepatic cholesterol, females accumulated more cholesteryl esters and less triacylglycerol, while males accumulated lower and more similar levels of cholesteryl esters and triacyglycerol. Consistent with these biochemical analyses, liver samples stained with osmium tetroxide and potassium dichromate to detect neutral lipids revealed increased lipid accumulation (lipid droplets) in livers from cholesterol-fed mice, especially female SCP-2 overexpressors. Conversely, in control-fed SCP-2/SCP-x null mice hepatic cholesteryl-esters and triacylglycerols, but not cholesterol, decreased by 50% (45). Control-fed SCP-x null mice also displayed a smaller, more complex pattern of reduced hepatic cholesteryl-esters and triacylglycerols (46).

Third, hepatic cholesterol accumulation induced by SCP-2 overexpression, especially in female mice, was associated with altered levels of receptors and/or receptor regulatory proteins involved in cholesterol uptake as follows: *i*) LDR-receptor levels were increased in response to SCP-2 overexpression. A major portion of cholesterol transported to the liver enters hepatocytes through the LDL-receptor pathway (1, 2). Increased expression of LDL-receptor together with decreased HMG-CoA reductase in the face of cholesterol and cholesteryl-ester accumulation suggested that SCP-2 overexpression contributed to the regulation of cholesterol homeostasis within the hepatocyte, i.e., toward decreased cholesterol synthesis and/or cholesterol esterification by ACAT2 in the endoplasmic reticulum whose level was also decreased in cholesterol-fed SCP-2 overexpressors. Conversely, while it was expected that SCP-2/SCP-x gene ablation would decrease LDL-receptor levels, control-fed SCP-2/SCP-x null mice exhibited unaltered LDL-receptor mRNA levels, likely due to compensation by L-FABP (upregulated) since control-fed L-FABP null mice show increased LDL-receptor levels (9, 37). *ii*) Levels of the HDL scavenger receptor SR-B1 were decreased in cholesterol-fed SCP-2 overexpressing mice concomitant with increased PDZK1 and MAP17 levels, proteins that regulate SR-B1 levels and its localization at the plasma membrane (reviewed in Ref. 7). Since the highest hepatic lipid

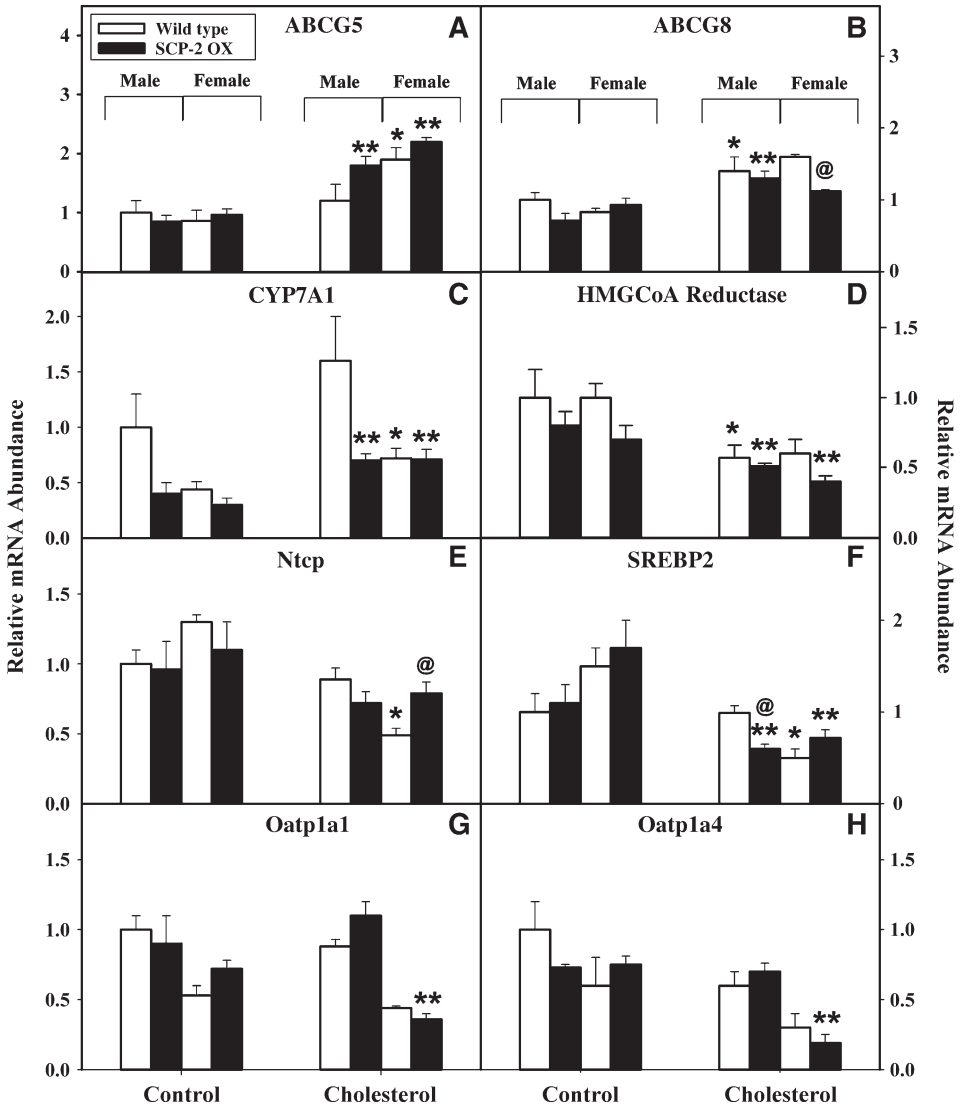

Fig. 10. Relative mRNA abundance of key enzymes involved in cholesterol homeostasis. Real-time PCR was used to determine relative mRNA abundance of the following enzymes: ABCG5 (A), ABCG8 (B), CYP7A1 (C), HMG-CoA reductase (D), Ntcp (E), SREBP2 (F), Oatp1a1 (G), and Oatp1a4 (H). Values represent means ± SEM (n = 5–7). * Indicates $P < 0.05$ versus WT mice on control diet; ** indicates $P < 0.05$ versus SCP-2-overexpressing mice on control diet; and the "at" symbol (@) indicates $P < 0.05$ versus WT mice on cholesterol-rich diet.

(cholesteryl ester, cholesterol, and triacylglycerol) occurred in cholesterol-fed SCP-2-overexpressing female mice, cholesterol retention was potentially facilitated by reduced HDL-mediated efflux concomitant with LDL-receptor-mediated cholesterol uptake. Furthermore, SR-B1 is a hepatic plasma membrane cholesterol-rich microdomain protein, able to redistribute between these microdomains and intracellular sites to maintain function (15). Consistent with this, livers from control-fed SCP-2/SCP-x null mice exhibited decreased levels of total SR-B1, but contained unaltered concentrations of SR-B1 in hepatocyte plasma membrane cholesterol-rich microdomains as well as increased total quantity of plasma membrane cholesterol-rich microdomains (15). Finally, MAP-17, as a canalicular PDZK1 binding protein, would be expected to reduce the level of SR-B1 (through destabilization of PDZK1) at the canalicular membrane where cholesterol efflux occurs, but not at the basolateral membrane where cholesterol uptake/efflux with serum HDL occurs (reviewed in Ref. 7).

Fourth, cholesteryl ester accumulation in control-fed SCP-2 overexpression mice was associated with selective increase in the hepatic expression of intracellular proteins that stimulate cholesterol esterification through transport (e.g., SCP-2 and/or L-FABP), yet not consistently with certain proteins associated with cholesterol esterification (ACAT2) or efflux (ABCA-1, ABCG5/ABCG8, and apoA1). SCP-2 and L-FABP are known to stimulate microsomal cholesterol esterification in vitro in the order SCP-2 > L-FABP (47). In transfected transformed cells overexpressing SCP-2 or L-FABP, cholesterol trafficking was stimulated from the plasma membrane to the endoplasmic reticulum where esterification occurs by ACAT (reviewed in Refs. 11, 18, and

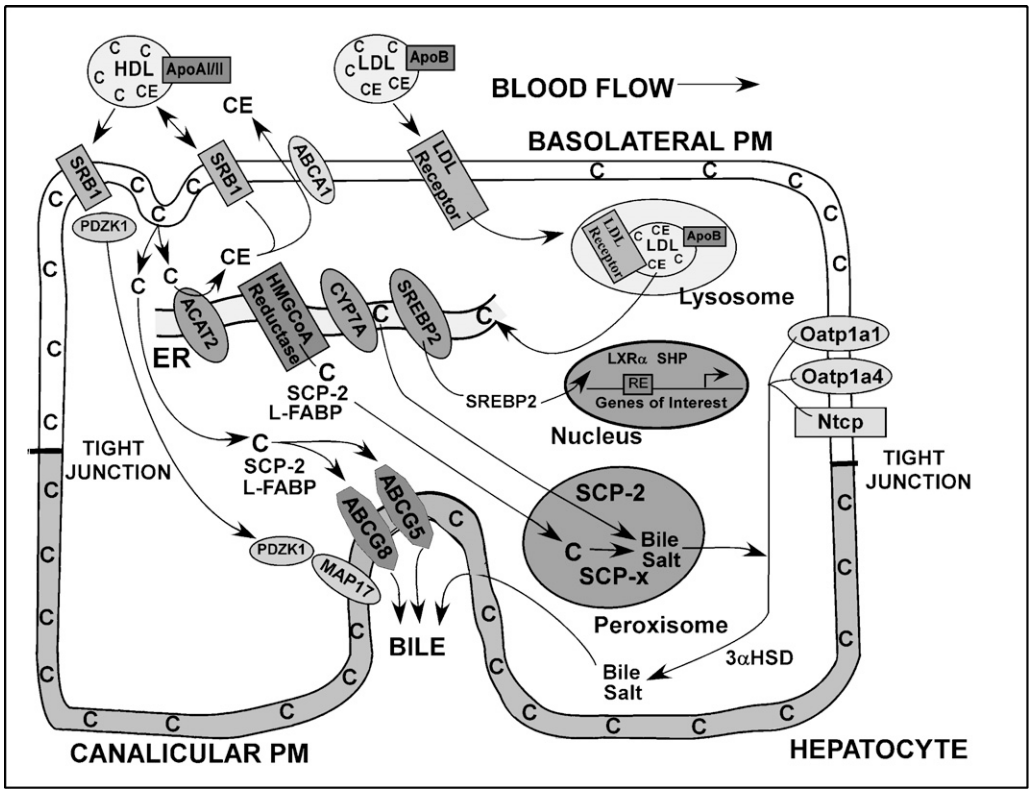

Fig. 11. Schematic diagram of hepatic cholesterol transport. Enzymes involved in cholesterol transport are illustrated. Plasma membrane (PM): Cholesterol enters the cell via the unidirectional LDL-receptor (present in clathrin-coated pits) (40) or the bidirectional HDL-receptor SR-B1 (located in caveolae/lipid rafts) (7). LDL-cholesterol (along with the receptor) is endocytosed as a clathrin-coated vesicle and fused to an acidic late endosome (lysosome) once the clathrin coat is shed. Cholesterol is released from the LDL-receptor, which can recycle back to the PM. HDL-mediated uptake/efflux of cholesterol SR-B1 is regulated by PDZK1 and MAP-17 (7). PDZK-1 is a scaffolding protein present at the basolateral and canalicular PM (7), while MAP-17, located at the canalicular PM, is thought to interact with PDZK1 and regulate its targeting to the PM (7, 41). ABCA-1, located at the basolateral PM, facilitates phospholipid desorption to apoA1 followed by cholesterol desorption to form HDL (reviewed in Ref. 8). Efflux through the canalicular PM into bile is facilitated by ABCG-5 and ABCG-8 (obligate heterodimers). Located at the basolateral PM are membrane proteins involved in bile acid binding/transport, including Oatp1a1, Oatp1a4, and Ntcp (42, 43). Cytosol: Several proteins bind/transport cholesterol to intracellular sites, including SCP-2 and L-FABP (reviewed in Refs. 8 and 18), while bile acid transport through the cytoplasm is facilitated by 3α-HSD (reviewed in Refs. 36 and 37). Endoplasmic Reticulum (ER): Enzymes involved in the rate-limiting steps of cholesterol and bile acids synthesis include HMG-CoA reductase and CYP7A1, respectively. ACAT mediates esterification of PM-derived cholesterol (reviewed in Refs. 36 and 37). SREBP2, regulated by cholesterol and coregulated by dietary fat, exists in two forms, a membrane-associated and a nuclear form (reviewed in Refs. 36 and 37). Nucleus: LXR-α and SHP are positive and negative transcriptional regulators, respectively, of the rate-limiting enzyme in bile acid synthesis (CYP7A1) and other enzymes of bile acid synthesis (reviewed in Refs. 36 and 37). Peroxisome: SCP-x, a branched-chain 3-ketoacyl-CoA thiolase, is involved in the oxidation of the branched side chain of cholesterol to bile salts (reviewed in Ref. 18).

48). Conversely, livers of SCP-2/SCP-x null mice exhibited reduced levels of cholesteryl esters, with unaltered ACAT2 levels (9, 45). With ABCA-1, ABCG5/ABCG8, or apoA1, proteins that facilitate cholesterol efflux, no consistent trend was observed with regard to SCP-2-mediated hepatic cholesterol accumulation. Moreover, SCP-2 overexpression had no affect on hepatic levels of ABCA1, ABCG5/ABCG8, or apoA1 in control-fed females, but levels of ABCA1 were decreased in control-fed males, results consistent with observed increases in cholesterol accumulation. In contrast, the cholesterol-rich diet increased levels of ABCA-1 in WT and SCP-2-overexpressing female mice, not in keeping with increased hepatic cholesterol levels observed with in these feeding groups. Similar trends were seen in ABCG5/ABCG8 expression levels, where the cholesterol-rich diet increased ABCG5 in male and female WT and SCP-2 overexpression mice, with a trend toward increased observed with ABCG8. Thus, while increased expression of SCP-2 and L-FABP, and to some extent ACAT2, potentially facilitated hepatic cholesterol accumulation, these results could not be predicted based on expression levels of ABCA-1, ABCG5/8, or apoA1, whose levels were unchanged or upregulated, especially in cholesterol-fed SCP-2-overexpressing mice.

Fifth, while SCP-2 overexpression had little effect on the hepatic levels of several enzymes involved in oxidation/transport of bile salts, including CYP7A1, CYP27A1, Ntcp,

Oatp1a1, and Oatp1a4, the effects of SCP-2 overexpression and cholesterol-rich diet were to increase levels of CYP7A1 and downregulate Oatp1a1, Oatp1a4, and SCP-x, the peroxisomal enzyme required for oxidation of cholesterol's branched side chain to produce bile acids. In addition, levels of serum and hepatic bile acids were decreased in cholesterol-fed SCP-2 overexpression mice, especially in female mice. While increased expression of CYP7A1 in the presence of decreased bile acids may seem counterintuitive, it should be noted that protein regulation is a complex mechanism. For example, under conditions of increased bile acid content, stimulation occurs of SHP, a transcriptional repressor that inhibits expression of several genes, including CYP7A1 and Ntcp, the major hepatocellular uptake system for bile acids (43). At low levels of bile acids, levels of SHP are reduced, promoting increased expression of CYP7A1 and Ntcp. Thus, increased expression of CYP7A1 and Ntcp in the presence of decreased bile acids is likely the result of downregulation of the orphan nuclear receptor SHP, yielding the trends observed for SCP-2 overexpression mice fed a cholesterol diet (decreased bile acids and upregulation of CP7A1 and Ntcp). Overall, bile induction of SHP provided a negative feedback inhibition of bile acid synthesis through bile acids (43). Thus, despite the concomitant upregulation of one or more other enzymes or nuclear receptors involved in bile acid synthesis, hepatic bile acid levels were decreased by SCP-2 overexpression in response to cholesterol enrichment, especially in female mice.

Sixth, the sexual dimorphic response of SCP-2 overexpression mice to a cholesterol-rich diet may in part be due to differential expression of key proteins involved in lipid metabolism under hormonal control. Sex-dependent differences in levels of several hepatic enzymes, proteins, and hormone receptors are well known and are brought about by the influence of androgenic and estrogenic hormones (49), the basis for which lies in the need of females to maintain reproductive competency for developing embryos where regulating steroid metabolism, lipid synthesis, and detoxification of waste products is essential. There is evidence that SCP-2 and SCP-x expression are regulated hormonally, since, as with other hepatic enzymes under androgenic control, sexual dimorphism of protein expression occurs after puberty and maturation of the pituitary gland (50). In addition, both the SCP-2 and SCP-x promoter regions contain putative estrogen response elements (51).

In summary, while the physiological function of one of the SCP-2/SCP-x gene products (SCP-x) in branched-chain lipid (phytol, cholesterol) metabolism has been resolved in both mice and man (9, 45, 46, 52), that for the other gene product (SCP-2) remained to be established. Earlier studies performed in vitro and in transfected transformed cells overexpressing SCP-2 have suggested a role for SCP-2 in cholesterol uptake, trafficking, metabolism, and efflux (reviewed in Refs. 11, 18, 48, and 53). In this work, key physiological questions, how sex, SCP-2 overexpression, and cholesterol-rich diet affect lipids and proteins involved in hepatic cholesterol homeostasis, were answered as follows: *i*) Female mice, especially cholesterol-fed SCP-2 overexpressors, exhibited the greatest changes in lipid and protein profiles, in keeping with hormonal control of several proteins involved in cholesterol metabolism. *ii*) Elevated levels of SCP-2 in the physiological range induced hepatic lipid (cholesterol/cholesteryl esters and triacylglycerol) and serum/biliary bile acid accumulation in control-fed mice. Hepatic cholesterol accumulation induced by SCP-2 overexpression was especially associated with increased levels of receptors involved in cholesterol uptake (LDR-receptor, HDL-receptor SR-B1, as well as PDZK1 and/or MAP17) and proteins involved in intracellular cholesterol trafficking (SCP-2 and/or L-FABP), without alteration of other proteins involved in cholesterol uptake (caveolin), esterification (ACAT2), efflux (ABCA-1, ABCG5/8, and apoA1), or oxidation/transport of bile salts (CYP7A1, CYP27A1, Ntcp, Oatp1a1, and Oatp1a4). *iii*) The effects of SCP-2 overexpression and cholesterol-rich diet were to downregulate proteins involved in cholesterol transport (L-FABP and SR-B1), cholesterol synthesis (related to SREBP2 and HMG-CoA reductase), and bile acid oxidation/transport (via Oapt1a1, Oatp1a4, and SCP-x, the peroxisomal enzyme required for oxidation of cholesterol's branched side chain to form bile acids). Consistent with these results, levels of serum and hepatic bile acids were decreased in cholesterol-fed SCP-2 overexpression mice, especially in females. Taken together, these findings indicate an important role for SCP-2 in hepatic cholesterol metabolism and homeostasis.

REFERENCES

1. Fielding, C. J., and P. E. Fielding. 1997. Intracellular cholesterol transport. *J. Lipid Res.* **38:** 1503–1521.
2. Chakravarthy, M. V., and C. F. Semenkovich. 2007. The ABCs of beta-cell dysfunction in type 2 diabetes. *Nat. Med.* **13:** 241–242.
3. Cohen, D. E. 1999. Hepatocellular transport and secretion of biliary lipids. *Curr. Opin. Lipidol.* **10:** 295–302.
4. Zanlungo, S., A. Rigotti, and F. Nervi. 2004. Hepatic cholesterol transport from plasma into bile: implications for gallstone disease. *Curr. Opin. Lipidol.* **15:** 279–286.
5. Dietschy, J. M., and S. D. Turley. 2002. Control of cholesterol turnover in the mouse. *J. Biol. Chem.* **277:** 3801–3804.
6. Everson, W. V., and E. J. Smart. 2005. Caveolae and the regulation of cellular cholesterol homeostasis. *In* Advances in Molecular and Cell Biology. M. P. Lisanti and P. G. Frank, editors. Elsevier, Amsterdam. 35–55.
7. Silver, D. L. 2004. SRB1 and protein-protein interactions in hepatic high density lipoprotein metabolism. *Rev. Endocr. Metab. Disord.* **5:** 327–333.
8. Schroeder, F., B. P. Atshaves, A. M. Gallegos, A. L. McIntosh, J. C. Liu, A. B. Kier, H. Huang, and J. M. Ball. 2005. Lipid rafts and caveolae organization. *In* Advances in Molecular and Cell Biology. M. P. Lisanti and P. G. Frank, editors. Elsevier, Amsterdam. 3–36.
9. Fuchs, M., A. Hafer, C. Muench, F. Kannenberg, S. Teichmann, J. Scheibner, E. F. Stange, and U. Seedorf. 2001. Disruption of the sterol carrier protein 2 gene in mice impairs biliary lipid and hepatic cholesterol metabolism. *J. Biol. Chem.* **276:** 48058–48065.
10. Fuchs, M., F. Lammert, D. Q. H. Wang, B. Paigen, M. C. Carey, and D. E. Cohen. 1998. Sterol carrier protein-2 participates in hypersecretion of biliary cholesterol during cholesterol gallstone formation in genetically gallstone susceptible mice. *Biochem. J.* **336:** 33–37.
11. Moncecchi, D., E. J. Murphy, D. R. Prows, and F. Schroeder. 1996. Sterol carrier protein-2 expression in mouse L-cell fibroblasts alters cholesterol uptake. *Biochim. Biophys. Acta.* **1302:** 110–116.
12. Baum, C. L., E. J. Reschly, A. K. Gayen, M. E. Groh, and K. Schadick. 1997. Sterol carrier protein-2 overexpression enhances sterol cycling and inhibits cholesterol ester synthesis and high density lipoprotein cholesterol secretion. *J. Biol. Chem.* **272:** 6490–6498.

13. Schroeder, F., A. A. Frolov, E. J. Murphy, B. P. Atshaves, J. R. Jefferson, L. Pu, W. G. Wood, W. B. Foxworth, and A. B. Kier. 1996. Recent advances in membrane cholesterol domain dynamics and intracellular cholesterol trafficking. *Proc. Soc. Exp. Biol. Med.* **213:** 150–177.
14. Atshaves, B. P., A. Gallegos, A. L. McIntosh, A. B. Kier, and F. Schroeder. 2003. Sterol carrier protein-2 selectively alters lipid composition and cholesterol dynamics of caveolae/lipid raft vs non-raft domains in L-cell fibroblast plasma membranes. *Biochemistry.* **42:** 14583–14598.
15. Atshaves, B. P., A. L. McIntosh, H. R. Payne, A. M. Gallegos, K. Landrock, N. Maeda, A. B. Kier, and F. Schroeder. 2007. Sterol carrier protein-2/sterol carrier protein-x gene ablation alters lipid raft domains in primary cultured mouse hepatocytes. *J. Lipid Res.* **48:** 2193–2211.
16. Parr, R. D., G. G. Martin, H. A. Hostetler, M. E. Schroeder, K. D. Mir, A. B. Kier, J. M. Ball, and F. Schroeder. 2007. A new N-terminal recognition domain in caveolin-1 interacts with sterol carrier protein-2 (SCP-2). *Biochemistry.* **46:** 8301–8314.
17. Zhou, M., R. D. Parr, A. D. Petrescu, H. R. Payne, B. P. Atshaves, A. B. Kier, J. A. Ball, and F. Schroeder. 2004. Sterol carrier protein-2 directly interacts with caveolin-1 in vitro and in vivo. *Biochemistry.* **43:** 7288–7306.
18. Gallegos, A. M., B. P. Atshaves, S. M. Storey, O. Starodub, A. D. Petrescu, H. Huang, A. McIntosh, G. Martin, H. Chao, A. B. Kier, et al. 2001. Gene structure, intracellular localization, and functional roles of sterol carrier protein-2. *Prog. Lipid Res.* **40:** 498–563.
19. Gallegos, A. M., S. M. Storey, A. B. Kier, F. Schroeder, and J. M. Ball. 2006. Stucture and cholesterol dynamics of caveolae/raft and non-raft plasma membrane domains. *Biochemistry.* **45:** 12100–12116.
20. Storey, S. M., A. M. Gallegos, B. P. Atshaves, A. L. McIntosh, G. G. Martin, K. Landrock, A. B. Kier, J. A. Ball, and F. Schroeder. 2007. Selective cholesterol dynamics between lipoproteins and caveolae/lipid rafts. *Biochemistry.* **46:** 13891–13906.
21. Atshaves, B. P., A. Petrescu, O. Starodub, J. Roths, A. B. Kier, and F. Schroeder. 1999. Expression and intracellular processing of the 58 kDa sterol carrier protein 2/3-oxoacyl-CoA thiolase in transfected mouse L-cell fibroblasts. *J. Lipid Res.* **40:** 610–622.
22. Atshaves, B. P., H. R. Payne, A. L. McIntosh, S. E. Tichy, D. Russell, A. B. Kier, and F. Schroeder. 2004. Sexually dimorphic metabolism of branched chain lipids in C57BL/6J mice. *J. Lipid Res.* **45:** 812–830.
23. Hogan, B., R. Beddington, F. Constantini, and E. Lacy. 1994. Manipulating the Mouse Embryo, a Laboratory Manual. Cold Spring Harbor Laboratory Press, Plainview, NY. 217–252.
24. Sambrook, J., E. F. Fritsch, and T. Maniatis. 1989. Molecular Cloning: A Laboratory Manual. Cold Spring Harbor Laboratory Press, Plainview, NY.
25. Adra, C. N., P. H. Boer, and M. W. McBurney. 1987. Cloning and expression of the mouse pgk-1 gene and the nucleotide sequence of its promoter. *Gene.* **60:** 65–74.
26. McBurney, M. W., S. Fournier, K. Jardine, and L. Sutherland. 1994. Intragenic regions of the murine PgK-e locus enhance integrationof transfected DNAs into genomes of embryonal carcinoma cells. *Somat. Cell Mol. Genet.* **20:** 515–528.
27. Kohli, A., R. Twyman, R. Abranches, E. Wegel, E. Stoger, and P. Christou. 2003. Transgene integration, organization, and interaction in plants. *Plant Mol. Biol.* **52:** 247–258.
28. Gutierrez-Adan, A., E. A. Maga, E. Behboodi, J. S. Conrad-Brink, A. G. Mackinlay, G. B. Anderson, and J. D. Murray. 1999. Expression of bovine beta-lactoglobulin in the milk of transgenic mice. *J. Dairy Res.* **66:** 289–294.
29. Atshaves, B. P., A. L. McIntosh, H. R. Payne, J. Mackie, A. B. Kier, and F. Schroeder. 2005. Effect of branched-chain fatty acid on lipid dynamics in mice lacking liver fatty acid binding protein gene. *Am. J. Physiol. Cell Physiol.* **288:** C543–C558.
30. Thigpen, J. E., K. D. Setchell, M. F. Goelz, and D. B. Forsythe. 1999. The phytoestrogen content of rodent diets. *Environ. Health Perspect.* **107:** A182–A183.
31. Hall, P., B. M. Gormley, L. R. Jarvis, and R. D. Smith. 1980. A staining method for the detection and measurement of fat droplets in hepatic tissue. *Pathology.* **12:** 605–608.
32. Hara, A., and N. S. Radin. 1978. Lipid extraction of tissues with a low toxicity solvent. *Anal. Biochem.* **90:** 420–426.
33. Bradford, M. M. 1976. A rapid and sensitive method for the quantitation of microgram quantities of protein utilizing the principle of protein dye binding. *Anal. Biochem.* **72:** 248–254.
34. Atshaves, B. P., A. L. McIntosh, O. I. Lyuksyutova, W. R. Zipfel, W. W. Webb, and F. Schroeder. 2004. Liver fatty acid binding protein gene ablation inhibits branched-chain fatty acid metabolism in cultured primary hepatocytes. *J. Biol. Chem.* **279:** 30954–30965.
35. Marzo, A., P. Ghirardi, D. Sardini, and G. Meroni. 1971. Simplified measurement of monoglycerides, diglycerides, triglycerides, and free fatty acids in biological samples. *Clin. Chem.* **17:** 145–147.
36. Martin, G. G., B. P. Atshaves, A. L. McIntosh, J. T. Mackie, A. B. Kier, and F. Schroeder. 2005. Liver fatty acid binding protein (L-FABP) gene ablation alters liver bile acid metabolism in male mice. *Biochem. J.* **391:** 549–560.
37. Martin, G. G., B. P. Atshaves, A. L. McIntosh, J. T. Mackie, A. B. Kier, and F. Schroeder. 2006. Liver fatty acid binding protein gene ablation potentiates hepatic cholesterol accumulation in cholesterol-fed female mice. *Am. J. Physiol. Gastrointest. Liver Physiol.* **290:** G36–G48.
38. Johnson, J. D., N. J. Bell, E. L. Donahoe, and R. D. Macfarlane. 2005. Metal ion complexes of EDTA as solutes for density gradient ultracentrifugation: influence of metal ions. *Anal. Chem.* **77:** 7054–7061.
39. Livak, K. J., and T. D. Schmittgen. 2001. Analysis of relative gene expression data using real-time quantitative PCR and the $2^{-\Delta\Delta CT}$ method. *Methods.* **25:** 402–408.
40. Brown, M. S., and J. L. Goldstein. 1986. A receptor-mediated pathway for cholesterol homeostasis. *Science.* **232:** 34–47.
41. Ikemoto, M., H. Arai, D. Feng, K. Tanaka, J. Aoki, N. Dohmae, K. Takio, H. Adachi, M. Tsujimoto, and K. Inoue. 2000. Identification of a PDZ-domain-containing protein that interacts with the scavenger receptor class B type 1. *Proc. Natl. Acad. Sci. USA.* **97:** 6538–6543.
42. Hagenbuch, B., and P. J. Meier. 2004. Organic anion transporting polypeptides of the OATP/SLC21 family: phylogenetic classification as OATP/SLCO superfamily, new nomenclature and molecular/functional properties. *Pflugers Arch.* **447:** 653–665.
43. Zollner, G., P. Fickert, D. Silbert, A. Fuchsbichler, C. Stumptner, K. Zatloukal, H. Denk, and M. Trauner. 2002. Induction of short heterodimer partner 1 precedes downregulation of Ntcp in bile duct-ligated mice. *Am. J. Physiol. Gastrointest. Liver Physiol.* **282:** G184–G191.
44. McArthur, M. J., B. P. Atshaves, A. Frolov, W. D. Foxworth, A. B. Kier, and F. Schroeder. 1999. Cellular uptake and intracellular trafficking of long chain fatty acids. *J. Lipid Res.* **40:** 1371–1383.
45. Seedorf, U., M. Raabe, P. Ellinghaus, F. Kannenberg, M. Fobker, T. Engel, S. Denis, F. Wouters, K. W. A. Wirtz, R. J. A. Wanders, et al. 1998. Defective peroxisomal catabolism of branched fatty acyl coenzyme A in mice lacking the sterol carrier protein-2/sterol carrier protein-x gene function. *Genes Dev.* **12:** 1189–1201.
46. Atshaves, B. P., A. L. McIntosh, D. Landrock, H. R. Payne, J. Mackie, N. Maeda, J. M. Ball, F. Schroeder, and A. B. Kier. 2007. Effect of SCP-x gene ablation on branched-chain fatty acid metabolism. *Am. J. Physiol. Gastrointest. Liver Physiol.* **292:** 939–951.
47. Chao, H., M. Zhou, A. McIntosh, F. Schroeder, and A. B. Kier. 2003. Acyl CoA binding protein and cholesterol differentially alter fatty acyl CoA utilization by microsomal acyl CoA: cholesterol transferase. *J. Lipid Res.* **44:** 72–83.
48. Murphy, E. J., and F. Schroeder. 1997. Sterol carrier protein-2 mediated cholesterol esterification in transfected L-cell fibroblasts. *Biochim. Biophys. Acta.* **1345:** 283–292.
49. Jost, A. 1953. Problem of fetal endocrinology: the gonadal and hypophyseal hormones. *Recent Prog. Horm. Res.* **8:** 379–418.
50. Roff, C. F., A. Pastuszyn, J. F. I. Strauss, J. T. Billheimer, M. T. Vanier, R. O. Brady, T. J. Scallen, and P. G. Pentchev. 1992. Deficiencies in sex-regulated expression and levels of two hepatic sterol carrier proteins in a murine model of Niemann-Pick type C disease. *J. Biol. Chem.* **267:** 15902–15908.
51. Ohba, T., J. A. Holt, J. T. Billheimer, and J. F. I. Strauss. 1995. Human sterol carrier protein x/sterol carrier protein 2 gene has two promoters. *Biochemistry.* **34:** 10660–10668.
52. Ferdinandusse, S., P. Kostopoulos, S. Denis, R. Rusch, H. Overmars, U. Dillman, W. Reith, D. Haas, R. J. A. Wanders, M. Duran, et al. 2006. Mutations in the gene encoding peroxisomal sterol carrier protein-x (SCP-x) cause leukencephalopathy with dystonia and motor neuropathy. *Am. J. Hum. Genet.* **78:** 1046–1052.
53. Atshaves, B. P., O. Starodub, A. L. McIntosh, J. B. Roths, A. B. Kier, and F. Schroeder. 2000. Sterol carrier protein-2 alters HDL-mediated cholesterol efflux. *J. Biol. Chem.* **275:** 36852–36861.